Available online at www.sciencedirect.com
ScienceDirect
Continental Shelf Research 27 (2007) 1317–1343
CONTINENTAL SHELF RESEARCH
www.elsevier.com/locate/csr

Resolution issues in numerical models of oceanic and coastal circulation

David A. Greenberg[a,*,1], Frédéric Dupont[b], Florent H. Lyard[c], Daniel R. Lynch[d], Francisco E. Werner[e]

[a]Fisheries and Oceans Canada, Bedford Institute of Oceanography, Dartmouth, Nova Scotia, Canada
[b]Québec-Océan, Université Laval, Québec, Québec, Canada
[c]LEGOS, CNRS, Toulouse, France
[d]Dartmouth College, Hanover, New Hampshire, USA
[e]University of North Carolina, Chapel Hill, North Carolina, USA

Received 1 February 2006; received in revised form 29 September 2006; accepted 9 October 2006
Available online 7 February 2007

Abstract

The baroclinic and barotropic properties of ocean processes vary on many scales. These scales are determined by various factors such as the variations in coastline and bottom topography, the forcing meteorology, the latitudinal dependence of the Coriolis force, and the Rossby radius of deformation among others. In this paper we attempt to qualify and quantify scales of these processes, with particular attention to the horizontal resolution necessary to accurately reproduce physical processes in numerical ocean models. We also discuss approaches taken in nesting or down-scaling from global/basin-scale models to regional-scale or shelf-scale models. Finally we offer comments on how vertical resolution affects the representation of stratification in these numerical models.

Keywords: Numerical ocean; Model; Resolution; Finite difference; Finite element; Coastline; Assimilation; Open boundary conditions; Topography

1. Introduction

Modelling the ocean will always involve compromises of scale. Even with increases in computation speed and available memory, any model is subject to practical limits on its resolution. This is true for all models, not just those with fixed resolution, but also those based on mapped Cartesian coordinates such as finite difference (FD) models, or variable triangle finite element (FE) or finite volume (FV) models. Increasing the spatial resolution, i.e. making the model's spatial grid size (Δx) smaller, generally increases requirements for computer storage space, memory and computation time. The increase in computational time results not only from the increased number of computation points, but also from the requirement to decrease the model time step (Δt) to satisfy various well known computational fluid dynamic stability criteria (e.g. Richtmeyer and Morton, 1967; Roache, 1976; Haidvogel

*Corresponding author. Tel.: +1 902 426 2431; fax: +1 902 426 6927.
E-mail address: davidgreenberg@alumni.uwaterloo.ca (D.A. Greenberg).
[1]Manuscript prepared while on research leave at LEGOS, CNRS, Toulouse, France.

0278-4343/$ - see front matter © 2007 Elsevier Ltd. All rights reserved.
doi:10.1016/j.csr.2007.01.023

and Beckmann, 1999; Kantha and Clayson, 2000; Lynch, 2005). For surface gravity wave problems propagating in a region of depth h, explicit in time computations are limited by the CFL stability requirement ($\Delta t < \Delta x/\sqrt{gh}$, where g is the gravitational acceleration and $\sqrt{gh}$ is the gravity wave speed) and implicit in time computations are limited by the Courant condition ($v\Delta t < \Delta x$, where v is the fluid velocity).

The scales important to an accurate numerical solution of a problem are not generally uniform over the domain of a model. Changes in bottom topography and coastline over small scales, as well as the presence of density fronts, eddies, etc., can have a critical influence over the processes throughout a domain that determine the required resolution. Similarly, if regular spacing in latitude and longitude is used in an ocean model covering higher latitude seas, the contraction of longitude lines towards the poles leads to distorted grid cells and different resolved scales in the north–south versus east–west directions.

In this paper we review certain aspects of spatial resolution requirements of oceanic circulation models and the approaches taken in specific applications. An issue related to the problem of resolution that we feel needs to be addressed first is the problem of open boundary conditions and nested grids. These arise when the small spatial scales addressed by regional models necessitate the truncation of larger domains, despite the large increase in computing power seen in the last four decades. Nested and variable resolution models are often part of the solution (Section 2). The second issue we address is the importance of properly resolving small channels and sills connecting larger bodies of water (Section 3). The third aspect is related to resolution problems found in models employing structured grids in resolving coastlines, i.e. the so-called staircase problem (Section 4). The fourth aspect is related to the bottom topography which needs to be accurately represented to properly simulate wave speed, steep slope processes and obstructions to flow (Section 5). Fifth, we discuss how resolving the baroclinic Rossby radius influences model solutions at basin-scales with an example of the North Atlantic (Section 6). Sixth, we present how data assimilation can yield misleading results when the important physical properties are not spatially resolved (Section 7). Seventh, we highlight aspects of mesh generation techniques presently used to prescribe model resolution requirements (Section 8). And finally, we look at some of the factors that make it difficult to resolve vertical ocean dynamics (Section 9). In our summary, we make a list of factors we suggest need to be considered in determining the resolution of circulation models (Sections 10 and 11).

2. Open boundaries and nested grids

The study of open boundaries and nesting meshes encompasses much more material than could reasonably be included in this review. Here we limit our discussion to pointing out different important aspects of the subjects and giving some entry points to the literature.

The treatment of open boundaries is an important issue, indirectly related to the models' resolution requirements. While numerical models of coastal and shelf regions may be capable of capturing details of the flow in domains of interest, they cannot afford to explicitly include the simultaneous solution of the larger neighboring basin-scale domain at appropriate levels of resolution. Similarly, basin-scale models cannot easily or affordably downscale to resolve the coastal regions. Presently, common practice is either to impose open boundary conditions on the regional models that allow for outward non-reflecting radiation of the computed solution (e.g. Orlanski, 1976; Chapman, 1985), implement "sponge-layers" along the open boundaries where the outward propagating signals are dissipated without reflection (e.g. Foreman et al., 2000), impose direct forcing on the open boundary from observations (e.g. Greenberg, 1979), or in some cases a combination of these (e.g. Flather, 1981; Werner et al., 1993b). Alternatively, boundary conditions extracted from basin-scale models are used to force (Hermann et al., 2002) or to provide best-prior estimates for the regional model (e.g. Lynch et al., 2001). An expanded domain using variable resolution, mapped coordinates (e.g. Haidvogel et al., 1991) or nested grids (e.g. Oey and Chen, 1992; Greenberg, 1979) is often used to further isolate the boundary effects from the core area, although nesting needs to be treated carefully (Davies and Hall, 2002). A different approach to considering the unmodelled ocean is taken in Garrett and Greenberg (1977) and Garrett and Toulaney (1979) where Green's functions are used to integrate model predictions with Platzman's (1975) normal modes for the Atlantic Ocean. This produced a correction to the computations done within the limited model domain and error estimates for remaining uncertainties.

The treatment of open boundaries in limited-domain models has been a persistent theme in ocean modelling (Orlanski, 1976; Camerlengo and O'Brien, 1980; Flather, 1981; Roed and Smedstad, 1984; Blumberg and Kantha, 1985; Chapman, 1985; Johnsen and Lynch, 1995; Lynch and Holboke, 1997; Palma and Matano, 1998; Penduff et al., 2000; Davies et al., 2003; Blayo and Debreu, 2005). Methods advanced in these papers have been fairly successful in keeping disturbances generated within the domain from reflecting at the boundaries and contaminating the solutions. However, care has to be taken to treat transient, oscillating and steady components correctly. Transient and periodic signals are often treated in some form of radiation condition that needs an outgoing speed for the component crossing the boundary. Steady and low-frequency components are frequently dealt with by considering across boundary gradients of elevation or currents that are in near geostrophic balance (e.g. Lynch et al., 1992; Werner et al., 1993a).

None of the above techniques will account for true interaction with the ocean outside the model domain or for forcing on the exterior ocean (e.g. meteorology) that will impact the boundary of the domain. The study of Hayashi et al. (1986) addressed the question of boundary influences on steady wind driven circulation in coastal ocean models. They showed that influences from an upstream boundary (in the sense of a shelf-wave), can be significant throughout the model and that assuming an infinite shelf upstream implies an unrealistic length of uniform shelf adjacent to that boundary.

The further the open boundary is from the area of interest, the less impact it will have on the desired solutions due to later arrival and increased damping in transit of errors propagated. Variable resolution and nested mesh models are often used to accomplish this. This is done by using a graded mesh of (usually triangular) elements where large elements in the far-field grade "smoothly" into the more highly resolved region of interest. Another approach is to use assimilation. By using assimilation techniques, boundary conditions as well as model parameters can be inferred using available data. This can be very powerful in hindcasting and nowcasting and with care, in prediction. However as will be shown in Section 7, this approach is not without pitfalls.

3. Channels and sills

Accurate representation of channels and sills that connect different bodies of water within a model domain is of critical, even fundamental, importance to obtaining meaningful simulations. In limiting situations of Cartesian discretization only one or two grid cells are available to describe a strait (Fig. 1). In this situation, the strait width must take values in a set of discrete numbers at the price of misrepresenting the width. (A different aspect of shoreline resolution is dealt with in Section 4.)

Even when the model coastline has a better fit, but is represented with minimal resolution (Fig. 2), it is difficult to simultaneously compute the appropriate water depth and cross-sectional area

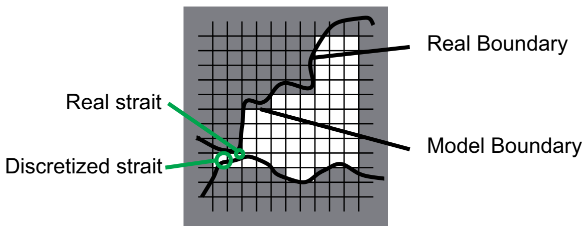

Fig. 1. Effect of a poor resolution on the geometry of a strait. This one is widened by about 100%. Straits are of great importance because they control the exchange of water between ocean basins.

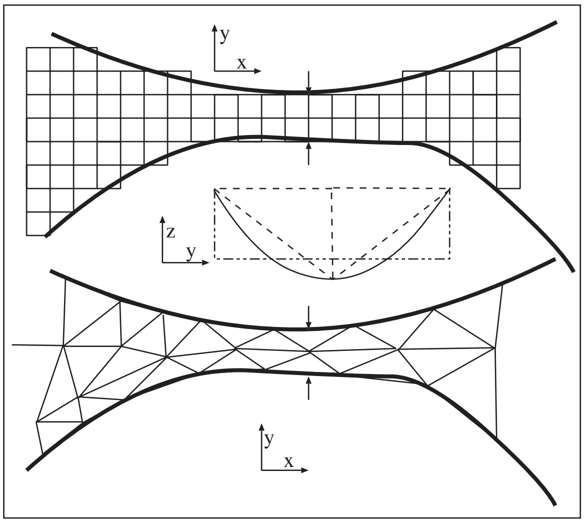

Fig. 2. Depending on the numerical scheme used, under-resolved channels in both finite element (below) and finite difference (above) schemes have problems representing simultaneously the depth and the cross-sectional area (center) leading to inaccurate determination of the transport.

correctly, leading to errors in phase speed and/or transport. As an example, in the Canadian Arctic Archipelago, Kliem and Greenberg (2003) found that the smaller channels make a significant contribution to the transport from the Arctic to the North Atlantic (Fig. 3). This requires resolution of order 1 km in a domain that spans 2000–3000 km.

The importance of resolution is also illustrated in cases where partially enclosed seas are linked to the ocean through restricted channels. Lake Maracaibo, in Venezuela, is an example of such a system. The lake is joined to the Gulf of Venezuela through narrow natural (and now also dredged) channels through Tablazo Bay and the Maracaibo Strait. To model the tides in this region, Molines et al. (1989) used three grids (one each for the Gulf of Venezuela, Tablazo Bay and Lake Maracaibo), with different mesh sizes and orientations, run independently, but using common tidal boundary conditions derived from observations. The system's tidal response obtained by Molines et al. (1989) was a composite of the three grids' solution, and found to quantitatively agree with observations only if different values of the bottom drag coefficient were specified in the various model sub-domains. Using a series of harmonic and time stepping FE models, Lynch and Werner (1987, 1991) and Lynch et al. (1990) considered tidal and baroclinic processes. Their model was able to concentrate high (and variable) resolution through the narrow straits, recovering the system's tidal response without requiring that different bottom drag coefficients be imposed. Lynch et al. (1990) showed that decoupling the Gulf from the Bay and the Lake produced a fundamentally different result for each sub-domain, than if the system were run as one single unit, thus establishing the importance of the explicit inclusion and resolution of the channels connecting the Gulf and Lake. A comprehensive study of exchange in the system was carried out by Laval et al. (2003) employing a FD model. To accommodate the variation in scales, they used some geometric straightening of the bathymetry to align with the mesh, and used a stretched computational grid focusing on the narrows. This permitted resolution as fine as 250 m and as large as 6 km. With this

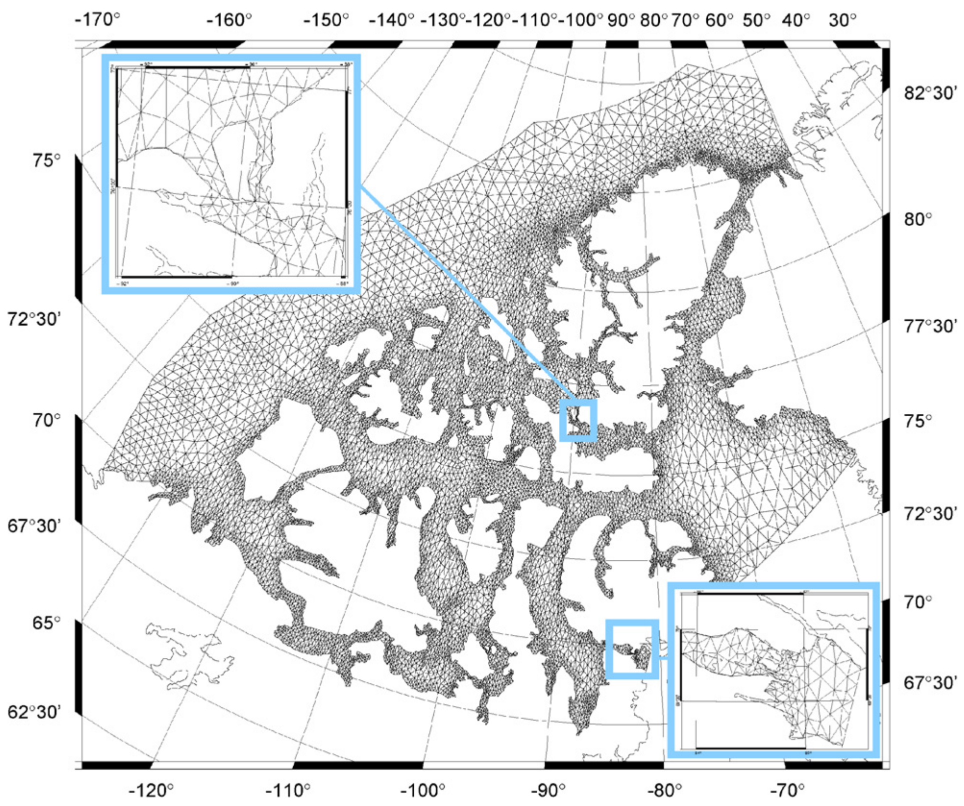

Fig. 3. In the Arctic Archipelago, Kliem and Greenberg (2003) found significant transport through the minimally resolved Fury and Hecla Strait (bottom) and Hellgate (top) channels.

model configuration they were able to produce a good picture of the balance between barotropic and baroclinic processes.

A situation physically similar to Lake Maracaibo is seen in the Bras d'Or Lakes, Nova Scotia, Canada. The Lakes are connected to the Cabot Strait and Atlantic Ocean via a shallow narrow passage. Within the Lakes, various basins are separated by sills and constrictions. Petrie (1999) and Petrie and Bugden (2002) have demonstrated that the frictional effects of the constricted channels effectively damp the diurnal and semi-diurnal tidal frequencies, but the longer period motions, mostly meteorological, originating outside the Lakes, propagate into the system largely unaffected. Tidal mixing is important to the observed hydrography. Dupont et al. (2003a) constructed a FE tidal model of the Lakes producing detailed solutions for five constituents, although some of the comparisons with the observations were not good, possibly due to short records and other data problems. Of interest, Petrie's (1999) simple model combining one-dimensional FD sections with rectangular basins gave a good qualitative picture of the response characteristics, damping the high frequencies and letting low frequency signals pass with minimal effect.

Whitehead (1998) identifies many deep passages and straits important to global ocean circulation. By considering the balance of the forces of pressure, Coriolis and inertia, together with hydrographic data, he was able to obtain a ''crude first approximation'' of some inter-basin fluxes. He felt that more realistic bathymetry is needed for better precision and posed several questions that should be addressed to better understand the local dynamics and therefore the larger picture. Similarly, Gille et al. (2004) commented on the problems ocean models have reproducing dense water overflows and the need for high-resolution bathymetry to accurately simulate them. They noted two areas, the Mid-Atlantic Ridge and the Indonesia Seas, where observations indicated fine scale processes leading to inter-basin exchange and found in some critical passages there have been no bathymetric surveys. Metzger and Hurlburt (2001) showed that when modelling the South China Sea at $1/16^{\circ}$ resolution, the inclusion of two shoals represented by individual topography grid points, had a major impact on the circulation through the Luzon Strait.

4. Resolving the coastline: the staircase problem

Some of the early studies advancing our fundamental understanding of large scale ocean dynamics were based on simple, most often rectangular, geometric forms—whereas the true basin geometry and coastline are more complicated. In FD models, the complexity of the geometry translates into the occurrence of steps along the discretized domain anywhere the orientation of the boundary does not correspond to that of the grid (Fig. 4). We hereafter limit ourselves to the case of the occurrence of steps along the lateral boundaries of the model.

It is important to note that for circular or smooth geometries it is possible to use curvilinear grids for FD methods and hence, avoid the occurrence of steps along the boundaries. Curvilinear grids can better fit irregular coastlines and can provide some variable resolution capabilities, such as implemented in the POM (Blumberg and Herring, 1987) and SPEM (Song and Haidvogel, 1994) models. However, for a realistic representation of lateral boundaries, step-like features would still appear since curvilinear grids only accommodate the large scale features of the coastline.

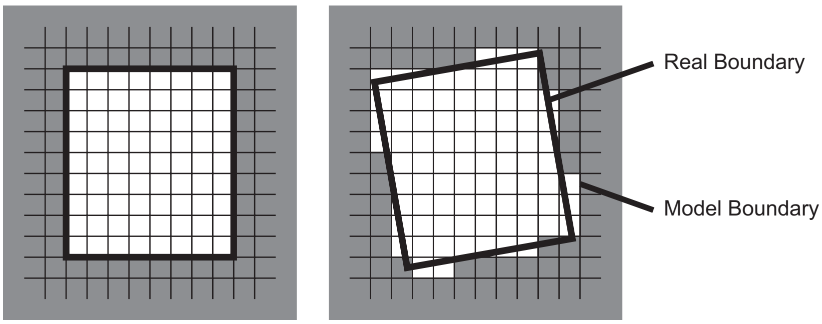

Fig. 4. Effect of the rotation on the discretization of a square domain. When the sides are not aligned with the axes, step-like features occur along the walls.

We first review the propagation of Kelvin waves in a rotated square basin. Then we review convergence problems found in the typical wind driven Munk problem but in a rotated square basin. Finally we show convergence rates for a wind driven circulation in a circular basin, for which an analytical solution can be derived.

4.1. The shallow water equations

We propose to solve idealized shallow water (SW) equations. While these equations are considerably simplified compared to the primitive equations, the dynamical processes involved in the formation of wind-driven circulation and the interaction with irregular coastlines are similar enough that we can restrict ourselves to these equations as an introductory study. The equations are

$$\partial_t \mathbf{u} + \mathbf{u} \cdot \nabla \mathbf{u} + f\mathbf{k} \times \mathbf{u} + g\nabla\eta = \frac{\boldsymbol{\tau}}{h} + v\nabla^2\mathbf{u}, \tag{1}$$

$$\partial_t \eta + \nabla \cdot (\mathbf{u}h) = 0, \tag{2}$$

where symbols are defined in Table 1. These equations correspond to a Boussinesq, hydrostatic, homogeneous ocean in which we assume that there is no vertical structure, reducing the real three-dimensional (3D) problem to a simpler two-dimensional (2D) problem. The acceleration due to gravity is here reduced with the goal of mimicking the first baroclinic mode dynamics, i.e. the dynamics of the upper layer of the ocean. The interlayer stress is taken to be zero, therefore no drag or bottom friction appears in Eq. (1). The wind stress $\boldsymbol{\tau}$ is the only external forcing applied.

4.2. Kelvin wave propagation along a steplike wall

From theoretical arguments, Mysak and Tang (1974) showed that Kelvin waves can be retarded by irregularities along a coastline. The effect is stronger for larger scale irregularities and not very significant for small scales. Pedersen (1996) studied the influence of steps on gravity waves and found this retardation effect at coarse resolution. This effect was also noted in circular lakes by Beletsky et al. (1997) for different kinds of staggering of the grid and vertical representations. Using different hierarchy of ocean models, Schwab and Beletsky (1998) found the same for Kelvin waves, the effect diminishing with higher resolution. These results are reproduced in Fig. 5 using a SW C-grid model based on Sadourny (1975). Four grids in total were used: two grids with no rotation of the basin showing no step along the boundaries at 10 and 5 km resolution and two grids with a 30° rotation of the basin relative to the discretization axes showing steps along the walls at also 10 and 5 km resolution. The finding that higher resolution decreases the retardation effect is consistent with the idea that Kelvin waves should not be sensitive to coastline details, at scales small compared to the Rossby radius of deformation. In Fig. 5, for the highest resolution runs (5 km), the retardation effect is still noticeable but it is much weaker compared to the runs at 10 km resolution. Since the radius of deformation is 31 km in these runs, these results imply that we should resolve the Rossby radius with about 10 points (when using a second-order formulation). One consequence for modelling the ocean is that the fast modes of an ocean basin (the Kelvin modes) will be misrepresented, especially if the model resolution is coarse. Therefore, transient responses of the ocean, such as the El Niño Kelvin wave along the Western America may be retarded, which may have consequences on the period of occurrences of El Niño events according to the delayed oscillator theory (Schopf and Suarez, 1988). For instance, in the study of Soares et al. (1999), there are only two points to represent the Rossby radius of deformation at 20° North.

In the context of the Munk problem, it is not clear how retarded Kelvin waves affect the steady state of the ocean. We propose to further investigate these issues in the context of the single gyre Munk problem in the next section.

4.3. Single gyre Munk problem in presence of steplike walls

In the classic single gyre Munk circulation with a constant wind, the sphericity and rotation of the

Table 1
Definition of variables in Eqs. (1) and (2)

(x, y, z)	The coordinate system (east, north, upward)
$\mathbf{u} = (u, v)$	Vertically averaged velocity
η	Elevation of the water surface taken from rest
h_b	Depth of the undisturbed water
$h = \eta + h_b$	Total depth of water
$\mathbf{k} = (0, 0, 1)$	Unit vector in the vertical
∇	Horizontal gradient operator
$f = f_0 + \beta y$	Coriolis parameter, f_0 and β defined at 45°
v	Dynamic eddy viscosity
$\boldsymbol{\tau} = (\tau_x, \tau_y)$	Wind stress in $m^2\,s^{-2}$

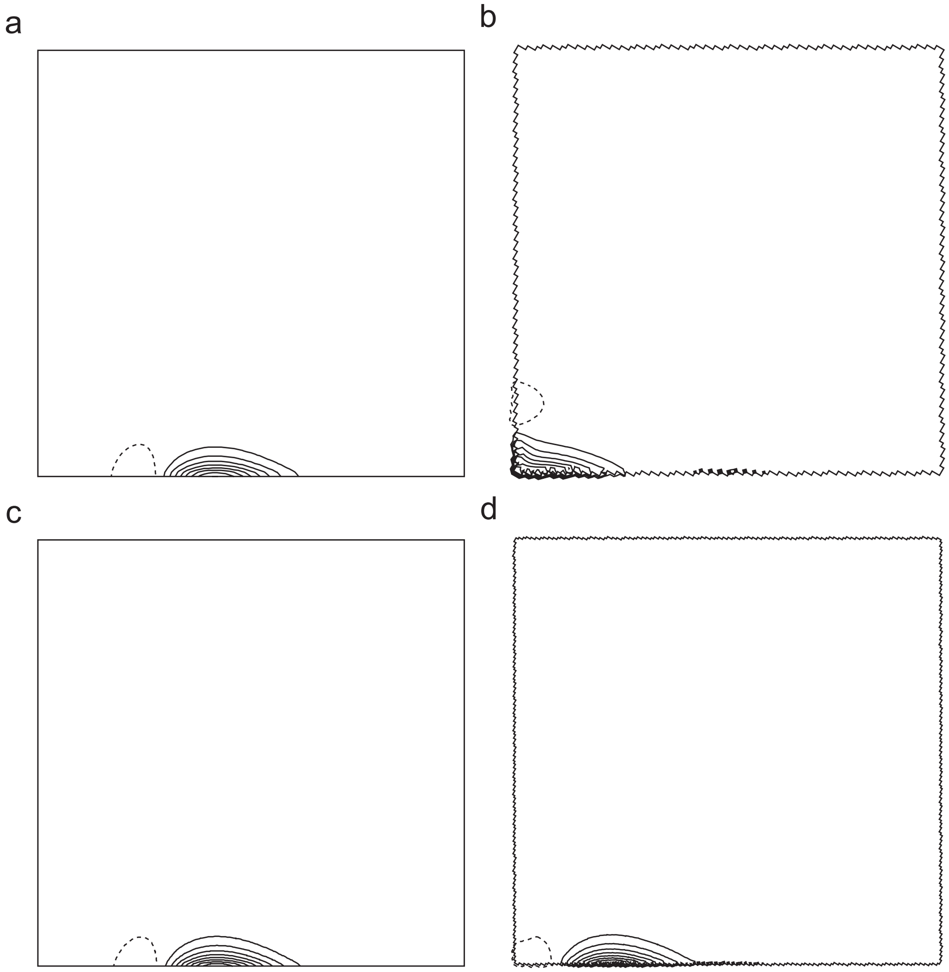

Fig. 5. Elevation field for the Kelvin retardation problem in the presence of steps along the walls at two different resolutions. α represents the rotation angle of the grid relative to the discretization axes. (a) 10 km, $\alpha = 0$; (b) 10 km, $\alpha = 30°$; (c) 5 km, $\alpha = 0$; (d) 5 km, $\alpha = 30°$. The dashed line is the -0.01 m contour, the solid lines are contours from 0.1 to 1.0 m with an increment of 0.1 m.

earth yield a strong return flow along the western wall ($\tau_x = -10^{-4}\sin(\pi(y/L_y))$ and $\tau_y = 0$). The energy put into the ocean by the winds is dissipated mainly in a viscous sublayer along the boundary because of the strong return flow there. A strong recirculation forms in the northwestern part of the domain, evidence of the non-linear effects in the solution.

Cox (1979), in the broader context of the circulation of the Indian Ocean, implemented some rotating experiments which showed that under no-slip boundary condition the circulation is not significantly modified by the presence of steplike walls. Adcroft and Marshall (1998), hereafter AM, conducted a thorough study of the impact of steplike walls for the single gyre Munk problem in presence of no-slip or free-slip dynamical boundary conditions using a C-grid SW model. Their results essentially confirmed Cox's results that the horizontal circulation under the no-slip boundary condition is not very sensitive to the presence of steps along the coastline. This may be explained by the fact that the core of the boundary current under no-slip is located a few grid points inside the interior of the basin.

For free-slip, however, they compared results from non-rotated and rotated square basin experiments and showed the circulation to be highly sensitive to the presence of steps along the walls. In rotated basin experiments, the basin was rotated relative to the grid axes (see Fig. 4), but the wind forcing and north–south axis were kept constant relative to the basin, so that the only differences between the experiments are due to the discretization. The presence of steps along the boundary tends to reduce the strength of the circulation to the extent that results obtained using free-slip boundary conditions with step-like boundaries more closely resemble those with no-slip boundary conditions than free-slip solutions without steps.

Moreover, they showed that, at least for small rotation angles, sensitivity to steps under free-slip conditions could be greatly reduced by using a vorticity–divergence formulation of the viscous stress tensor (Madec et al., 1991) instead of the conventional five-point Laplacian operator. The two tensor formulations are equivalent in a non-rotated basin, but are different in presence of steps. Around steps, the vorticity–divergence formulation tends to accelerate the fluid parcels compared to the conventional stress formulation. Fig. 6 reproduces the basic ideas of AM after 6 years of integration from rest. The combinations are for the FD model with the enstrophy conserving advective scheme of Sadourny (1975) and with, respectively (A) the conventional stress tensor (five-point) and (B) the vorticity–divergence stress tensor of Madec et al. (1991). The figure shows the elevation fields for the A and B cases and for no rotation and a small rotation angle of 3.4°. Clearly, the A case shows circulation patterns collapsing as the number of steps along the walls increases whereas, for the B case, the circulation is quite similar to the original non-rotated circulation.

Dupont et al. (2003b) investigated further the problem by computing vorticity budgets for the whole basin in presence of steplike walls. The numerical budget is actually not defined up to the model coastline due to the large footprint of the model vorticity equation used in the C-grid staggering. Without going into excessive detail, this means the model vorticity budget allows for some advective flux to leave or enter the domain. This advective flux can then be used as a measure of the convergence of the model since it usually tends to zero in non-rotated domains following the discretization order given by the vorticity (1 for a second-order accurate FD model). However, due to the increased number of steps and the high value of the advective flux around steps, it is no longer obvious that the advective contribution to the vorticity budget goes to zero as the resolution is increased in rotated square basins. They found that combination A (and other combinations) do not show evidence of convergence, contrary to combination B. In the latter case, the convergence order of the advective contribution is close to one (the maximum allowable for vorticity in a primitive second-order FD model, and by extension any residual present in the vorticity budget of such a model) irrespective of the rotation angle but with the curve shifted to larger values.

The effect of staircases on the coastal dynamics can also be felt via the appearance of spurious vorticity/divergence extrema. Spiky vorticity/divergence may imply spurious local upwelling/downwelling. Dupont et al. (2003b) discussed the relevance of their results in the perspective of 3D modelling. One application is to large scale z-level models where the lateral walls can be significant (for instance at a sharp shelf slope between a shallow shelf and a deep ocean) and may be sufficient for the mechanism introduced herein to dominate even in the presence of a whole variety of other physical processes. Section 9 examines further, the problem of representing the local dynamics in the presence of lateral and vertical staircases, which may well explain the relative difficulty z-level models have in representing some slope dynamics (Mellor et al., 2002).

4.4. An inviscid wind-driven circulation in a circular domain

A linear analytical solution can be found for the wind-driven problem in a circular domain with Coriolis forces and damped by a linear bottom friction. No viscosity is included. There is a no-normal flow condition at the model boundary and the wind forcing is similar to the Munk gyre case. The steady state for the linearized SW solution in polar coordinates is

$$\eta = \frac{W}{4gHR}xy \tag{3}$$

and with Coriolis force:

$$\eta = \frac{Wf}{RgH\kappa}\left[\frac{R^2}{8} + \frac{1}{4}\left(\frac{\kappa}{f}xy - (x^2+y^2)\right)\right]. \tag{4}$$

We perform a one year run from rest for all models with windstress, $W = 10^{-4}\,\mathrm{m^2\,s^{-2}}$, $f = 10^{-4}\,\mathrm{s^{-1}}$ or zero, $g = 10^{-2}\,\mathrm{m\,s^{-2}}$, the basin radius, $R = 500\times 10^3\,\mathrm{m}$, uniform depth, $H = 1000\,\mathrm{m}$ and linear bottom friction coefficient $\kappa = 10^{-3}\,\mathrm{s^{-1}}$. This is

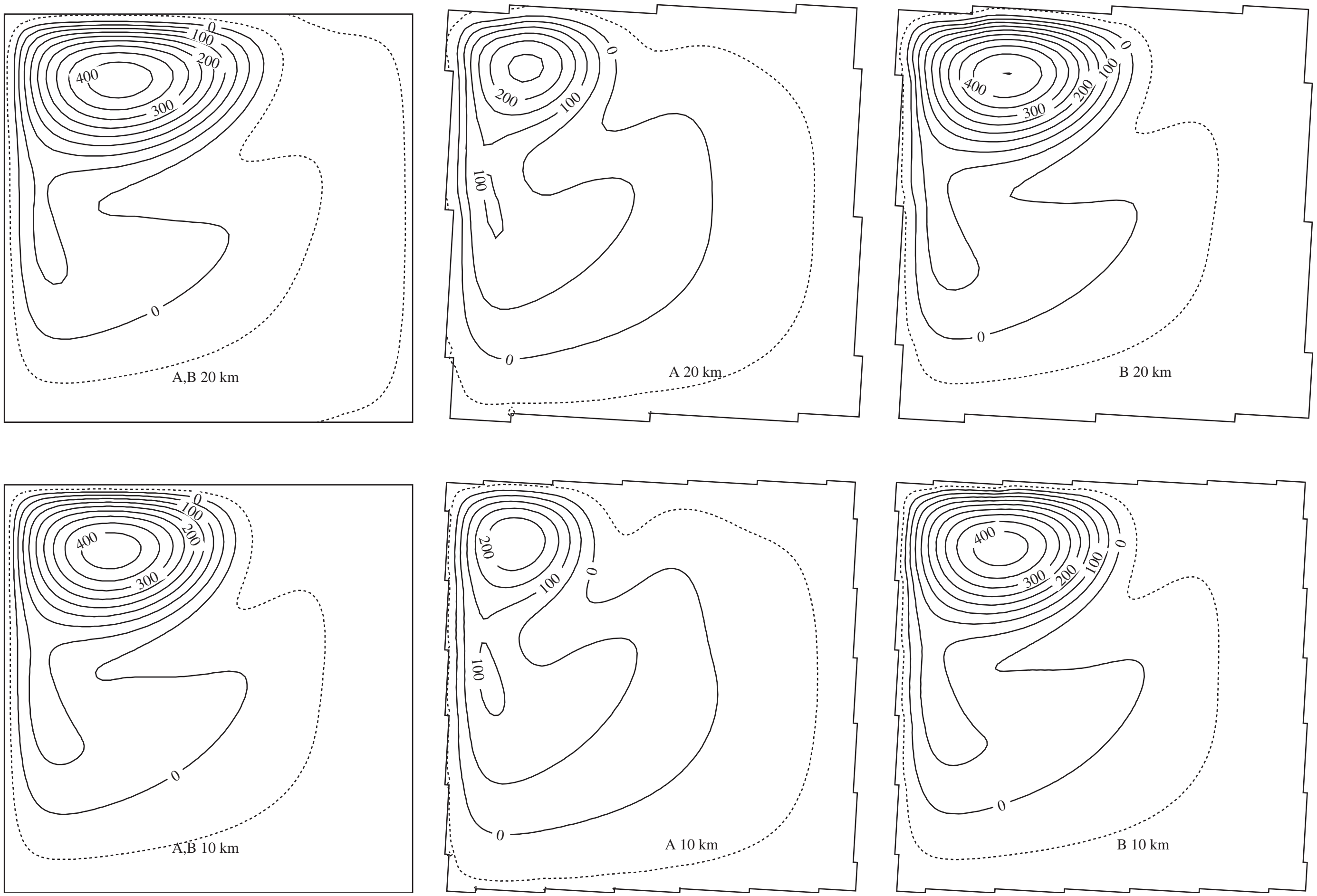

Fig. 6. Layer thickness in meters after a 6 year spin-up for 20 and 10 km resolution. Shown are results from the A and B combination (see text) with or without a 3.44° rotation angle of the basin. Note that the B case tends to resemble the A,B case with no rotation, but the A case does not.

enough to converge to a steady state. The normalized error is computed as

$$E(\eta_{mod}) = \frac{\int\int |\eta_{mod} - \eta|\,\mathrm{d}x\,\mathrm{d}y}{\int\int \mathrm{d}x\,\mathrm{d}y}\sqrt{\frac{\int\int \mathrm{d}x\,\mathrm{d}y}{\int\int \eta^2\,\mathrm{d}x\,\mathrm{d}y}}. \qquad (5)$$

We first analyze the results from the C-grid model. For brevity, we only show the results for one case, at $f = 0$, since convergence properties are not significantly different than those at $f \neq 0$. Fig. 7 shows the convergence of the normalized error in η with increasing resolution. It appears that the convergence order of the C-grid FD model is closer to one (1.1 when $f = 0$ and 1.3 when $f = 10^{-4}\,\mathrm{s}^{-1}$) than two, the maximum for this second-order FD formulation.

We also consider the solution from a fourth-order A-grid model (Dietrich, 1998). The original formulation, hereafter O-FDM4, however, uses second-order numerics close to the boundary. A modified version, R-FDM4, remains fourth-order by use of non-centered operators in the vicinity of the walls for derivatives oriented perpendicular to the walls. This modification was motivated by more accurate (and depending on the test-case, more stable) results when using this fourth-order extension. We now compare the solution from the C-grid FD model with the O-FDM4 and R-FDM4 models. Fig. 7 shows that the order of the A-grid model is actually less than two in the presence of step-like walls. Furthermore, there is no longer a difference, in terms of truncation order, between the second-order C-grid and the fourth-order A-grid models—

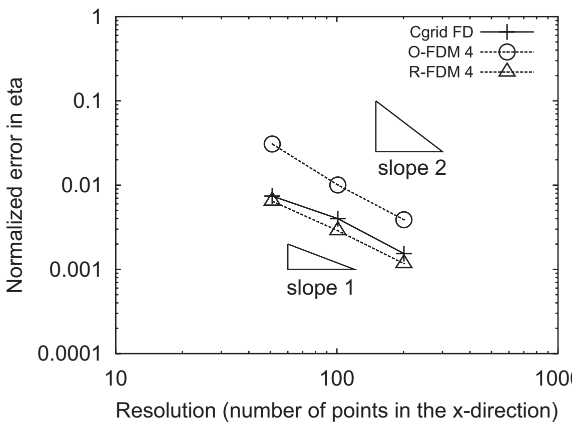

Fig. 7. Convergence with resolution of the normalized elevation error for the second order C-grid FD, O-FDM4 and R-FDM4 models in a circular domain.

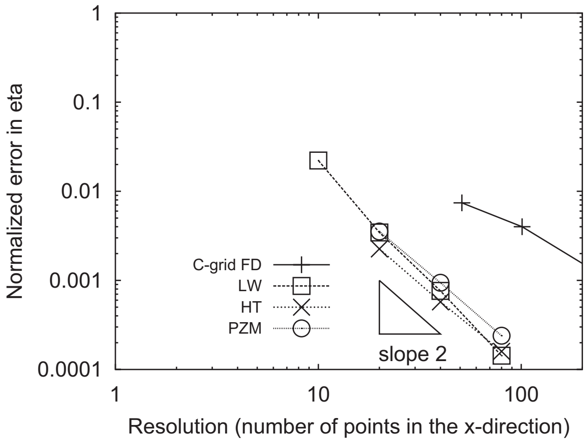

Fig. 8. Convergence with resolution of the normalized elevation error in a circular domain for three FE models (LW, HT, PZM) and the C-grid FD for comparison.

unlike the case with straight walls. Therefore, the presence of steps along irregular boundaries has a detrimental effect on the accuracy of high order FD formulations if the flow is allowed to slip along the walls.

We now compare three FE models to the C-grid model. This first FE model (Lynch and Werner, 1991) is based on equal order basis functions for pressure and velocity (also known as P_1-P_1) and on the generalized wave equation, hereafter referred as the LW model. The second (Hua and Thomasset, 1984) is based on non-conformal basis function for velocity (also known as $P_1^{NC}-P_1$), hereafter referred as the HT model. The last (Peraire et al., 1986) is based on a Taylor–Galerkin approximation using a P_1-P_1 approach, hereafter referred as the PZM model. In this circular geometry, all FE models have the advantage that the representation of the boundary improves as the resolution is increased. Therefore, it should be possible to observe convergence order close to two. Fig. 8 shows that all FE models have a convergence rate close to second-order. Hence in terms of accuracy, all FE models appear to perform better than FD models in non-rectangular geometries for linear inviscid problems.

5. Bottom topography and slope

5.1. The open ocean

The most elementary numerical considerations lead one to conclude that resolution of the operative horizontal wavelength must be respected. In SW dynamics, the wave speed is $\sqrt{gH}$ and hence one seeks uniform Courant number $(\Delta t/\Delta x)\sqrt{gH}$ as a metric of uniform truncation error. The classic findings of second-order accuracy in FD and FE methods require constant wave speed to justify uniform discretization. Over realistic topography, the generalization would be to keep the depth-dependent Courant number constant. Foreman (1984) suggested that this be a rule for graded meshes: effectively, for uniform Δt, $\Delta x^2 \sim H$. The same conclusion is reached in the frequency domain, where the applicable time scale is the inverse frequency $1/\omega$, and the applicable Courant number $\sqrt{gH}/\omega\Delta x$. In terms of tidal period P, the constraint becomes

$$\Delta x \leqslant \frac{P\sqrt{gH}}{n} \tag{6}$$

with n the number of nodes per wavelength. n is found typically to be in the range [20–100]. Le Provost et al. (1995) report $n = 30$ for simulation of global ocean tides. This general idea, modified for nearshore realism, remains a popular contemporary meshing rule (e.g. Jones and Davies, 2005).

It is easy to conclude from the above that very large Δx emerges over deep water. But at the shelf break and across isolated banks, there is more at stake in the gradient of H. And simple topographic fidelity demands higher resolution along real coasts, especially recognizing the ecological importance of transport processes there.

5.2. *The shelf break and bank sides*

Additional constraints on resolution have been observed to be operative in areas of steep topography. Loder (1980) called attention to the topographic length scale $H/\nabla H$ and the presence of circulation features at this scale in tidally rectified solutions on bank sides. Especially at subtidal timescales, these features are critical to bank ecology and proper resolution of this length scale would appear to be essential to those studies. The practical requirement becomes $\Delta H/H$ must be controlled on a per-grid box (per-triangle) basis:

$$\frac{\Delta x}{H}\frac{\Delta H}{\Delta x} = \frac{\Delta H}{H}. \tag{7}$$

Studies of subtidal circulation around Georges Bank by Lynch et al. (1995) have generally corroborated this with $\Delta H/H$ in the range [0.1–1].

The same consideration has been found operative for subtidal motions at the shelf break. Hannah and Wright (1995) compared analytic solutions with FE ones, and found the practical requirement $\Delta H/H < 0.3$ to avoid dominant errors at the shelbreak.

One can get the scale $(1/H)\partial H/\partial x$ readily by manipulating the vertically averaged continuity equation, with $\partial/\partial y = 0$, yielding:

$$\frac{1}{HU}\frac{\partial \zeta}{\partial t} + \frac{1}{U}\frac{\partial U}{\partial x} + \frac{1}{H}\frac{\partial H}{\partial x} = 0. \tag{8}$$

An order-of-magnitude analysis reveals that for tidal motions and steep topography, the transient term is small and hence a good approximation is

$$\frac{\partial U}{\partial x} = -\alpha U$$

with $\frac{1}{\alpha}$ the topographic length scale: $\alpha = \frac{1}{H}\frac{\partial H}{\partial x}$. (9)

Hence we expect length scales in the velocity solutions of order $1/\alpha$ driven externally by the topography. Their resolution will require mesh constraints of the form $\alpha\Delta x < 1$.

The Atlantic shelfbreak region has been studied extensively in the development of the ADCIRC model for the prediction of tide and storm surge along the Atlantic and Gulf coasts. The domain in these studies includes the Atlantic basin, shelf, and coast west of the 60°W meridian, including the Carribean Sea and the Gulf of Mexico (see Fig. 9). Westerink et al. (1995) found simple Courant-number-based mesh grading to be inadequate by itself. Overriding that was the finer resolution required in the shelfbreak region, where a practical requirement of tidal accuracy demanded 20 nodes in crossing the shelf break/slope region.

Luettich and Westerink (1995) discussed the critical issue of *bathymetric* resolution used in conjunction with hydrodynamic resolution. The presence of poorly resolved bathymetric features in hydrodynamic simulations is generic and confounds the study of convergence if new bathymetric features emerge as Δx is refined. Accordingly, systematic tidal studies demonstrate these effects separately. Even when subgrid topography has little observable impact in the tide-band, Lynch et al. (1995) found that it can seriously affect tidally rectified, residual flows.

Xing and Davies (1998) examined the Malin–Hebrides shelfbreak at high resolution, 2.4–4.6 km,

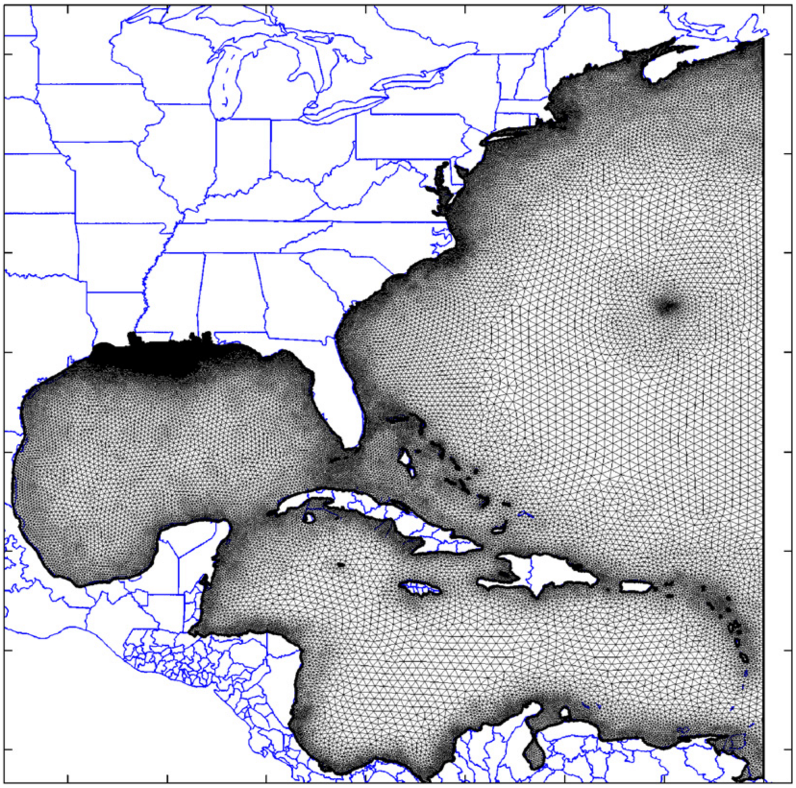

Fig. 9. The ADCIRC domain for tide and surge prediction. Approximate latitudinal range is 7°–46°N, and longitudinal range is 60°–97°W.

in order to describe internal tides generated there. Further studies on 2D cross-shelf transects used 0.6 km resolution to examine these phenomena in detail, and the interaction of tidal rectifaction and wind, and mixing (Xing and Davies, 2001, 1997). Hall and Davies (2005b) highlighted the value of variable resolution in this context. In addition they called attention to the importance of mesh-dependent subgrid-scale closure. Three-dimensional FE results demonstrate these effects on realistic Malin Shelf geometry (Hall and Davies, 2005a).

Blain et al. (1998) provide additional resolution studies which generally corroborate the ADCIRC findings; the context of hurricane prediction adds the requirement of resolving the scale of the storm model forcing, which can be severe on otherwise large Δx over deep water.

Smith (2005) found it necessary to resolve local ridges and troughs under 1 km in width, in order to capture the tide power distribution ($|v|^3$) suitable for power generation studies. An example appears in Fig. 11 wherein this effect is resolved within a regional (far-field) tidal context.

5.3. At the coast

As one approaches the shore, the bottom shoals and horizontal shear is generated via variable bottom stress in very SW. In reality this is the mechanism of "horizontal stress". The latter must be either mimicked by compensating horizontal boundary conditions on an imaginary sea wall, or the actual physics simulated by proper resolution of the actual topography. The resolution demands so generated far exceed those from the wavelength-resolution in the open ocean or from the topographic length scale on steep topography. Implied in topographic realism is fidelity to along-shore as well as cross-shore topography.

The nearshore area is in fact where much of the operational data are located. Blanton et al. (2004) studied the ADCIRC domain with both coarse and fine nearshore resolution along the Georgia/South Carolina coast. There, the presence of a dense estuary/tidal inlet complex (ETIC, Fig. 14) was found to be highly dissipative and affects the regional energy balance for the semidiurnal tides

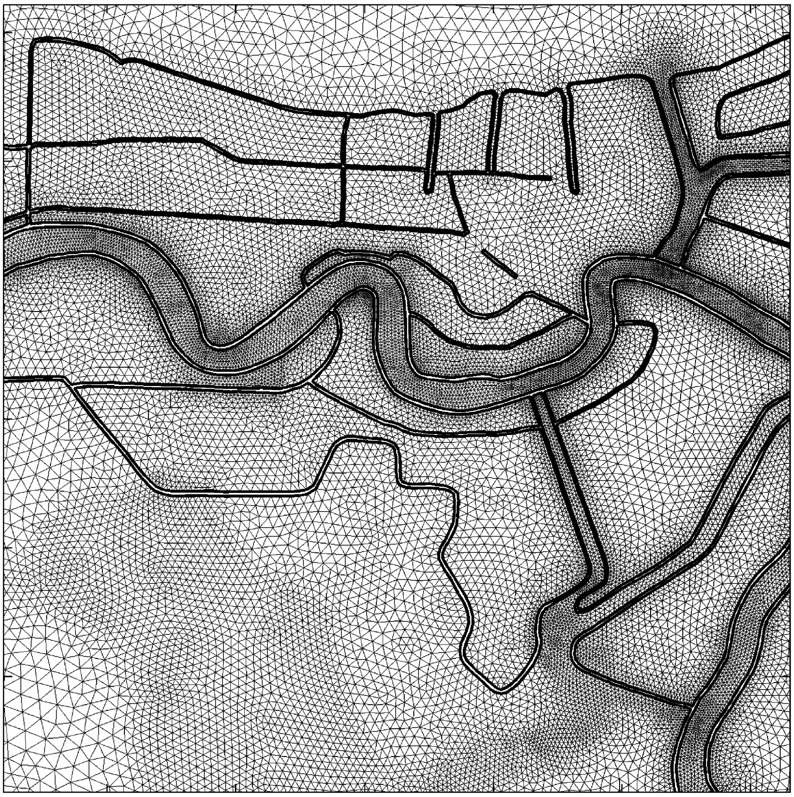

Fig. 10. Portion of ADCIRC mesh covering the city of New Orleans. This local resolution provides quality hurricane surge prediction when appended to the wide-area domain illustrated in Fig. 9. The horizontal scale of the figure is approximately 30 km per side.

(Fig. 15). This was found to affect regional skill assessment and to confound the interpretation of tidal data there unless properly resolved (Fig. 16).

Prediction of hurricane surge has been demonstrated using the collection of the expertise represented here (large domain, resolution of barotropic and topographic length scales, coastal resolution) in Blain et al. (1998). The significant extra demand is the propagation of tide and storm surge inland, which requires unusual topographic resolution for effective prediction. An example of this meshing is illustrated in Fig. 10.

5.4. *Shelfbreak and seamounts—baroclinic*

Resolution issues where topography varies rapidly were already addressed above in the context of barotropic flows. In the broader context of the baroclinic (density driven) flows, topographic features generate much smaller flow scales at the order of the deformation radius (see next section) and smaller, e.g. internal waves and tides, flow rectification due to tides (Wright and Loder, 1985) or interactions with the large scale circulation as in Taylor columns (Haza, 2004). At the shelf edge, internal waves and tides are generated and propagate both offshore and inshore. Those propagating offshore are the main concern here as they can travel long distances before being damped or breaking (e.g. Alford, 2003). These features are difficult to resolve and poses a major challenge to realistic state-of-the-art basin-scale circulation models since they still cannot afford to resolve the necessary 10 (or more) points for wavelike structures at the scale of the first deformation radius (Treguier et al., 2005). For the foreseeable future, selective filters—e.g. the Smagorinsky viscosity scheme for variable or stretched grids, where the viscosity essentially varies with the local resolution (Hall and Davies 2005a, b)—might be necessary to ensure model stability in regions of strong baroclinic process generation and/or propagation. As Hall and Davies (2005b) also show the improvements of the baroclinic tidal flow as the resolution is increased locally around seamounts and shelf breaks, it provides an interesting argument in favor

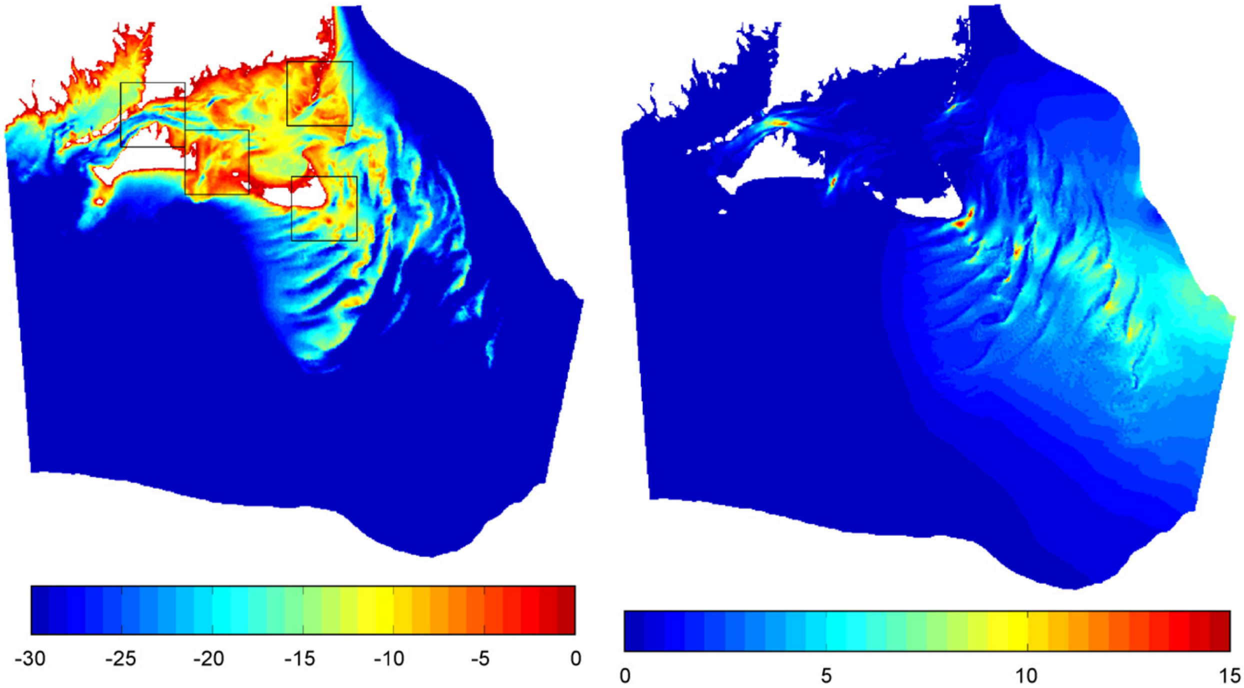

Fig. 11. (Left) Bathymetry (m) south of Cape Cod, MA. The resolution is 0.1–1 km. The square zoom boxes shown are length 20 km. (Right) Computed M2 power density, $\rho|\overline{V}|^3H/2$ [kw/m^2].

of variable resolution such as inherent of FE and FV models.However, even in FE/FV models, CFL constraints put practical limits on the smallest scales resolvable and baroclinic processes would limit the upper scales as well: just like in FD models, the first baroclinic radius of deformation would dictate the upper limit of Δx in a state-of-the-art FE model.

Cornillon (1986) first reported that infrared observations did not show evidence of changes in Gulf Stream properties upstream versus downstream of the New England seamounts. A more recent study (Ezer, 1994), using the Princeton Ocean Model (POM) looked at the Gulf Stream characteristics in absence and presence of the New England seamounts. He found in his numerical experiments that these seamounts had a southward deflection effect but surprisingly had a stabilizing impact on the Gulf Stream. Compared to the case where they are absent, seamounts cause the eddy kinetic energy to be smaller both upstream and downstream and the mean kinetic energy to be larger downstream. This modification of the upstream characteristics is indicative of propagating waves or trapped waves of large scale. Note, however, that Ezer's model was not run for longer than a year of simulated time. More recent altimetry measurement taken over 12 years (Fig. 1 of Dupont et al., 2006), shows a slight northward deflection of the field of surface elevation variance close to the seamounts. Finally, Haza (2004) in her thesis, stresses the importance of the New England seamounts in the bifurcation of the Gulf Stream and the increase in magnitude of the Slopewater Jet (Pickart et al., 1999). Although more work is required with varying resolution, it illustrates that seamount issues cannot be easily discarded for large scale circulation studies and that probably both upstream and downstream direction would require the best resolution possible.

6. The Rossby radius

The barotropic Rossby radius of deformation has been computed on the Lyard et al. (2006) mesh used for global tidal computations (Fig. 12). Even in shallow seas of polar latitudes the radius is very large, typically greater than 100 km. This should not be a factor in determining the resolution of global, basin or regional-scale models.

In contrast to the above, the fundamental importance of the first baroclinic Rossby radius of deformation (λ_1) to global ocean dynamics is described in the Chelton et al. (1998) study of the λ_1 global climatology. Because λ_1 depends on stratification, which varies over time, they looked

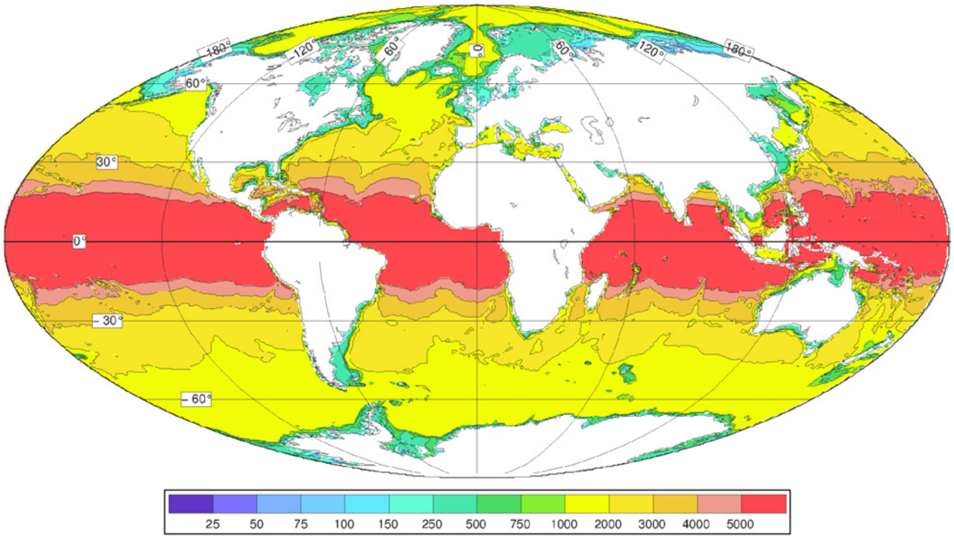

Fig. 12. The barotropic Rossby radius (km) as calculated on the global FE mesh of Lyard et al. (2006). For most computations, this would not be a factor in determining model resolution.

at the significance of this variation to the ocean dynamical computations. They found that the larger range variability in stratification was limited to the top few hundred meters so the full depth integral of the buoyancy frequency, used in λ_1 computation, was not greatly changed. They concluded that temporal variability was not significant for most considerations. They computed λ_1 on a global $1^\circ \times 1^\circ$ mesh. Of interest is that the lowest contour shown is 10 km ($\approx 0.09^\circ$ latitude) and that in the critical Gulf Stream–North Atlantic Current area between 40° and50° λ_1 was close to 20 km ($\approx 0.18^\circ$ latitude). Because we are interested in resolving the shorter length scales, we would like to look in more detail at the near polar values. Chelton et al. (1998) computational results are available online (http://www.coas.oregonstate.edu/research/po/research/chelton/index.html). We have plotted these in Fig. 13 for the northern North Atlantic and Antarctic. (Not all values are represented in these plots due to artifacts in the graphical display that shrink the domain around boundaries and missing grid points.) In the North Atlantic, λ_1 is seen to decrease to less than 5 km east of Greenland before increasing again northward. Around Antarctica, λ_1 is seen to be less than 7.5 km over a large area.

Smith et al. (2000) and Bryan et al. (2007) looked at how resolution affected computations of the North Atlantic Ocean. They showed how their 0.1° model greatly improved the eddy characteristics and the time averaged currents in comparisons with the simulations made with model resolutions of $\frac{1}{2}^\circ$ and $\frac{1}{6}^\circ$. The Gulf Stream and North Atlantic Current (see *note added in Proof* in Smith et al., 2000) separate from the continental shelf topography in the correct areas. Similarly, Maltrud and McClean (2005), using a global model with the same 0.1° resolution were able to produce good global eddy characteristics, but there were some anomalies and they had poorer results with the separation of the Gulf Stream.

The resolution necessary to include proper representation of λ_1's influence in ocean models is complex. Stammer (1997), looking at satellite data, found a strong empirical relationship between eddy scales at all latitudes and λ_1. A zonal average of eddy scales estimated from TOPEX data between latitudes -60° and $+60^\circ$ indicated the largest eddy scales were close to 100 km around the equator and diminished to 50–60 km near $\pm 60^\circ$. Cushman-Roisin (1994) points out how the relationship between the first Rossby radius and the meso-scale baroclinic instability typically has ratio of order greater than 1. He describes how in the case of the thermal wind flowing inside an ocean with constant Brunt–Väisälä frequency, N, i.e. the density is logarithmic, the stability limit is close to $2.6\lambda_1$. Under this limit, perturbations are not able to take the main stream circulation away from equilibrium, thus they are not able to capture potential energy

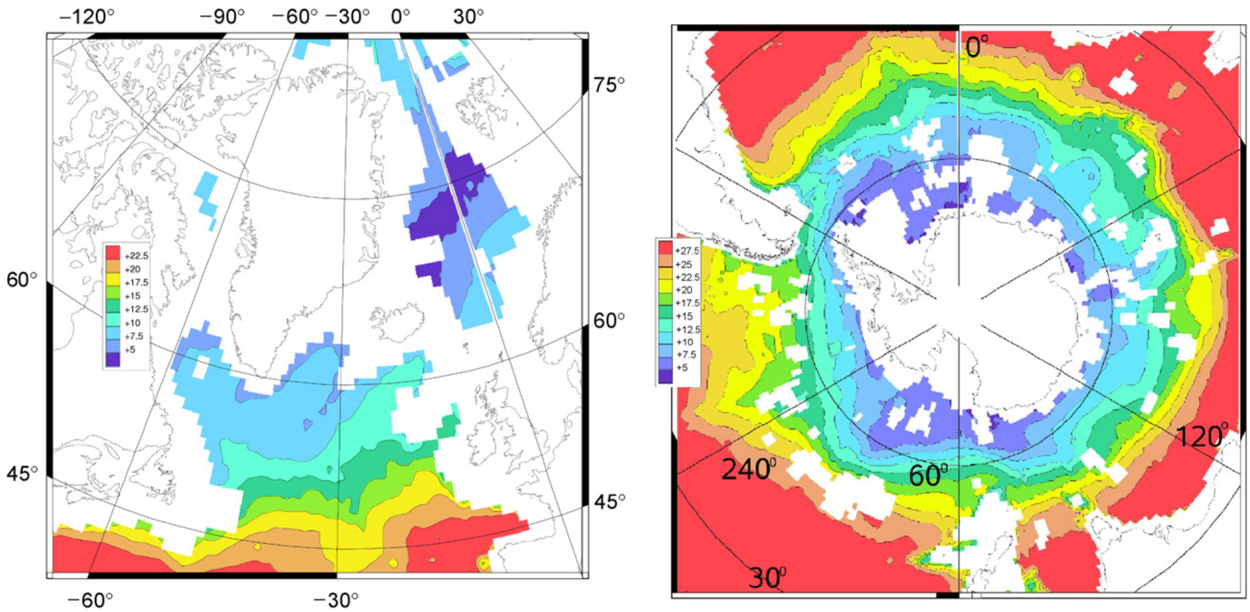

Fig. 13. Contours of the baroclinic Rossby radius (km) from Chelton et al.'s (1998) values obtained from the web (see text) for the northern North Atlantic (left) and the Antarctic (right).

from it, and consequently they do not have a significant interaction or effect on the main current. Within the range of wavelengths compatible with mesoscale instabilities, the fastest growing modes are the instabilities with wavelength close to $3.9\lambda_1$. These modes will capture most of the potential energy available from the mean thermal-wind circulation, and therefore are probably the most important to resolve properly.

Thus models might aim to resolve scales of $2.6-3.9\lambda_1$. Once these modes are resolved, as far as Rossby radius dynamics are concerned, there will be limited benefit in increasing resolution. What is the correct subsample of the length scale necessary for resolution? Coastline considerations (Section 4.2) would indicate a factor of $\frac{1}{10}\lambda_1$ being necessary. In Section 5.1 we note that a factor of $\frac{1}{30}$ of the wavelength seemed to define a reasonable resolution for the semi-diurnal tides. With λ_1 being less than 20 km and even less than 10 km in regions of considerable dynamic importance this would imply resolution of order 1 km ($\approx 0.009^\circ$ latitude) or even better. Such refinement is not practical in the foreseeable future for fixed or variable resolution models. Yet we note that Smith et al. (2000), Bryan et al. (2007), and Maltrud and McClean (2005) are approaching very reasonable circulation and turbulent energy characteristics with a resolution that is of order $1\lambda_1$. We believe we will need further model experimentation and understanding of the dynamical processes to resolve this.

7. Data assimilation

Even simple barotropic problems are poorly posed in practice. Demands of mesh extent normally push the boundaries further and further from the shore, where quality data are harder to find. The accumulated studies corroborate that the barotopic mode becomes less dissipative, and propagates faster, as we go further offshore. The wisdom of simulating as much of these phenomena as possible, ultimately encounters difficulty in prescribing seaward boundary conditions.

Several demonstrations have been made whereby the seaward BCs are deduced, ideally relative to a prior estimate, in order to make a simulation fit available data (e.g. Lynch et al., 1998; Lynch and Hannah, 2001; Lynch and Naimie, 2002). This is what we mean by data assimilation here. It is interesting that the most reliable operational data are typically found shoreward, and often in sensitive topographic locations. In those instances, there will be a near-field effect of the coastal topography. Failure to resolve this will result in false estimation of the far-field forcing. Instead, serious local truncation errors will be accommodated by creating far-field, boundary-forced errors which permeate the shelf.

The ETIC region of the South Atlantic Bight (mentioned above in Section 5.3) is a classic example. In Lynch et al. (2004), it was found that sub-km coastal resolution was required in order to make valid inference of boundary conditions as far offshore as the 70 m isobath. Failure to resolve the ETIC resulted in forecast errors equal in magnitude to the subtidal phenomena under study (Figs. 14–16). Worse, these errors are masked by a false confidence gained from 'fitting' a poorly resolved model to available data—errors are annihilated by the data assimilation at the observation points, but created elsewhere, all over the shelf.

8. Mesh generation

Since the recognition that variable resolution is within reach, there has been considerable interest in algorithms for mesh generation.

The FD method has been adapted by first inventing a mapping from the original Cartesian or polar coordinate system to a more natural, curved coordinate system (e.g. Blumberg et al., 1985, 1993). The mapping terms are then embedded in the governing PDE, which is discretized on regular grid in the mapped space. The problem of mesh generation is transferred to that of generating the coordinate transformation. As typically conceived, this approach involves a global coordinate transformation, a formidable task for all but the simplest transformations; and a numerical challenge in itself.

In the FE arena, this mapping approach is embedded in essentially all methods which use unstructured grids. The formalism developed in the FE arena is the "isoparametric transformation", and the principles here are (a) make the mapping *local*, definable on each FE independently of the others; (b) start in the natural numerical space (e.g. the triangle) and map outwards to the physical space; (c) concentrate on the level of continuity at the triangle boundaries; and (d) make the mapping easily automated at the element level. The most common form of this requires C^0 continuity, i.e. a polynomial map which is continuous across element boundaries, with first derivatives non-continuous there. And the most elementary form of this amounts to linear mapping over each triangle. The genius of this idea is that the map is conceived at the local, discrete level, and hence computable, in terms of simple local functions; while alternate ideas conceive a continuous global map which is then discretized along with the PDE.

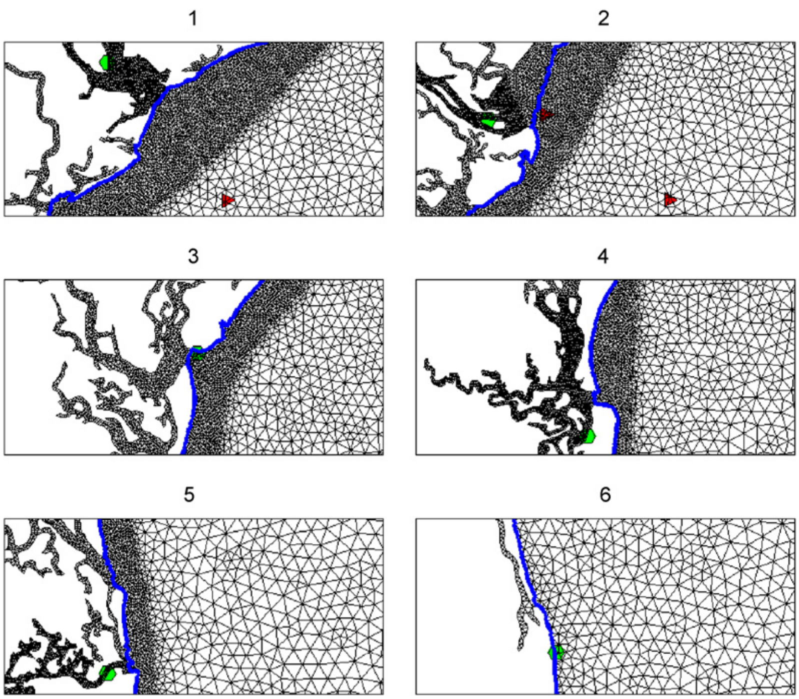

Fig. 14. Nearfield mesh resolving the ETIC, and data locations.

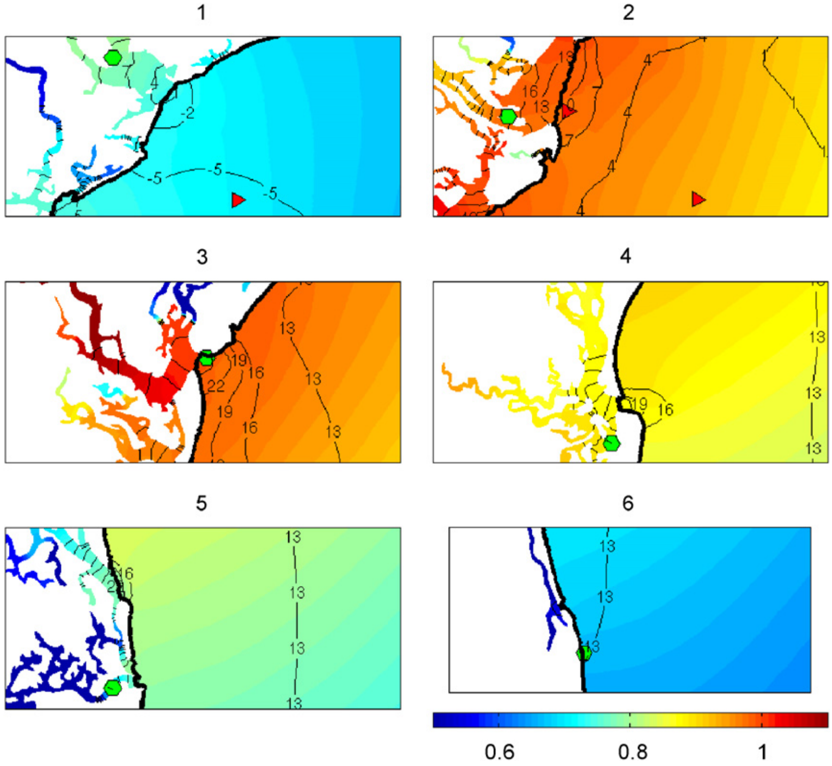

Fig. 15. Data-assimilative solution for nearfield M2 tidal amplitude (m) for the numbered areas identified in Fig. 16.

With unstructured grids, most common is the use of Delaunay triangulation of generated nodes, and subsequent refinement in various ways. This area remains a subjective art, as no extant algorithm provides fully satisfactory, reproducible results, and all attempts rely in the last analysis on heuristic, interactive adjustment.

An early example of unstructured mesh generation was presented by Henry and Walters (1993). This method generated triangles with the Courant constraint operative, resulting in uniform gravity wave resolution over variable topography. Examples of more complex generation of meshes on vastly different scales can be seen in Greenberg et al. (2005), Kliem and Greenberg (2003), and Lyard et al. (2006) which used unpublished software (*Lyard*) derived initially from the Henry and Walters (1993) TriGrid package.

More recently, Bilgili et al. (2005) describe a generator which incorporates a user-directed selection of several refinement criteria. Included are

- Element area.
- Topographic length scale resolution ($H/\nabla H$).
- H: shallow refinement.
- Uniform $1/\nabla H$.
- Wavelength resolution.
- Peclet number.
- Maximum slope.
- Relaxation by local averaging.

Like other methods in its class, this approach is typical in that it proceeds from coarse to fine grid, through selective refinement.

Hagen (2001), Hagen et al. (2000, 2001, 2002), and Hagen and Parrish (2003) have contributed the local truncation error analysis (LTEA) approach. In this approach, one seeks to make the truncation error uniform across the whole domain. Required is a high-resolution solution U, capable of being differentiated up to fifth-order. With these derivatives everywhere, one estimates the leading truncation error as

$$\varepsilon = \Delta x^2 \left[\frac{\partial^5 U}{\partial x^5}, \ldots \right] \tag{10}$$

which is different everywhere. By setting this to a constant everywhere, one gets a recipe for the local Δx, and proceeds to generate a coarser mesh. The

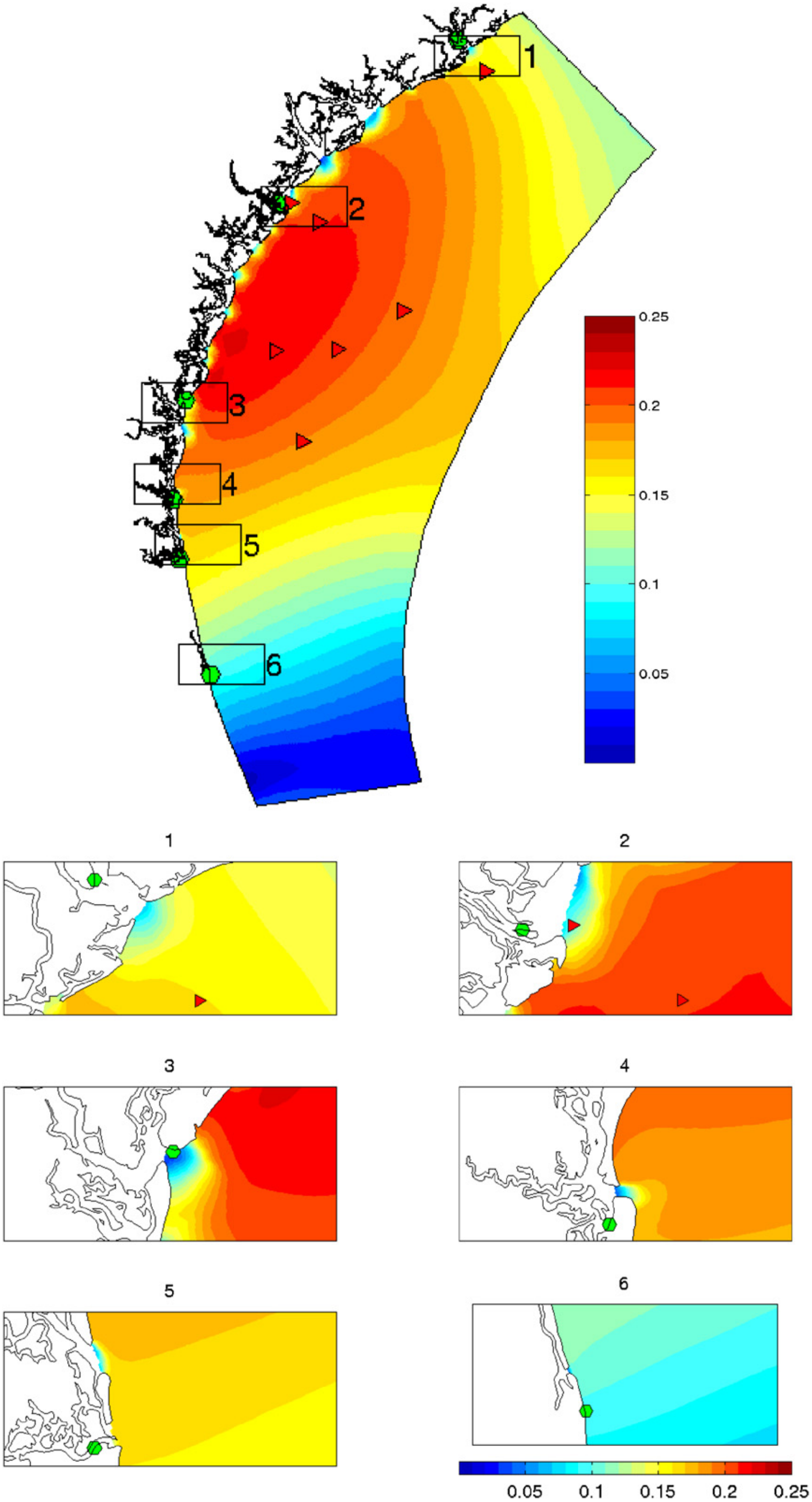

Fig. 16. Difference (m) between the ETIC-resolving and non-resolving solutions, following data assimilation. The results are plotted on the coarser mesh, which covers roughly 420 km along-shelf and 100 km cross-shelf. The difference is of order 20 cm over a significant portion of the shelf. The difference is vanishingly small at the data locations (green filled hexagons), as these points are fit to the model.

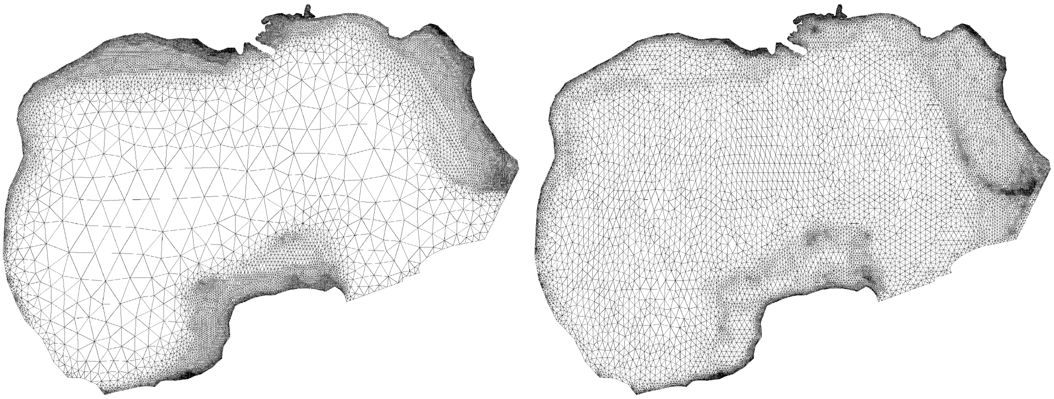

Fig. 17. Gulf of Mexico meshes from Hagen et al. (2001), (their Figs. 2 and 7, used with permission). The grid on the left was produced using a wavelength criterion and the grid on the right with LTEA (localized truncation error analysis). The meshes have approximately the same number of nodes and elements. Approximate latitudinal range is 18°–30.5°N, and longitudinal range is 81°–97°W.

difference between resolution based on the wavelength resolution and LTEA is seen in Fig. 17, Gulf of Mexico grids, (from Hagen et al., 2001, Figs. 2 and 7, used with permission). With approximately the same number of elements and nodes, the LTEA grid produced much smaller truncation errors and better agreement when tides computed with these meshes were compared with those from a higher resolution model.

Carey (1995) describes the classic *a posteriori* mesh refinement idea. Classic FE methods normally require setting the integral of the PDE imbalance (residual) to zero, weighted by the basis. As the integral represents an average at the element scale, hence the integrand (residual of the PDE) is only *weakly* zero, i.e. it is locally averaged to zero. The *posterior* procedure is to generate a coarse solution, estimate its weakness by evaluation of the residual's size (e.g. the per-element maximum) and use this as a criterion for mesh refinement: refine the peaks of the residual. In spirit, this is similar to the LTEA method, although going from coarse to fine, not the opposite.

There is a vast frontier of opportunity for automating mesh generation procedures and criteria in ways which give reproducible results and satisfy the collected concerns described here.

9. Issues in vertical resolution

It is difficult to imagine simulating vertical ocean processes without parameterizing significant pieces. We can think of the complex, but not rare, situation where there is a co-occurrence of a thermocline, solitons, tidal frequency internal waves, isopycnals that intersect the surface and the bottom, a surface Ekman layer from wind stress and a frictional bottom boundary layer. Resolving these vertical advective and diffusive motions on scales consistent with accurate computation of horizontal diffusion and advection remains a challenge. We note that global barotropic tidal computations needed to account for energy dissipation from internal tides to get optimal calibration (Lyard et al., 2006). They found that the independent estimates of this dissipation both in calibrating the model and in balancing the energy in assimilated solutions were very close in magnitude.

The staircase problem, described in Section 4 also arises in the vertical discretization of the topography in three-dimensional FD and FE models of the ocean. In models of the Bryan–Cox type (Bryan, 1969) based on the primitive equations, the vertical axis is discretized at various constant depths. They are called leveled or z-coordinate models. In these models, the topography follows a step-like representation and therefore they are prone to problems similar to the ones mentioned above (Section 4). For instance, the equivalent difficulty in z-coordinate models to the description of straits is the description of sills. The depth of sills or other important topographical features has to be taken from a set of discrete depths. It was realized early on that this step-like representation had negative effects on the overall circulation. For instance, z-coordinate models have meridional circulations which are known to be sensitive to the details of how the bottom boundary is represented. The issue is that they do not accurately advect denser waters along slopes and overestimate diapycnal mixing (Gerdes, 1993; Roberts et al., 1996; Roberts and Wood, 1997).

Different strategies have been proposed to circumvent the problem. One strategy was to change the vertical coordinate, z, to a terrain following coordinate, σ (Phillips, 1957; Blumberg and Mellor, 1983), Song and Haidvogel (1994). But σ-coordinate models encounter other known limitations, such as pressure gradient errors and artificial diapycnal mixing (e.g. Haney, 1991; Mellor et al., 1994). A second strategy is to use a layered (or ρ-coordinate) model (Bleck, 1978; Bleck and Boudra, 1981). Roberts et al. (1996) compared the behavior of the simulated North Atlantic in a z-model and in an isopycnal model (ρ-model). In particular, they noted that the z-model has more trouble in representing a realistic outflow from the Greenland basin (GIN). Roberts and Wood (1997) extended the study by systematically studying the effect of modifying the topography of the sill at the outflow of GIN and noted the high sensitivity of the model. The same observation was made by Winton (1997) in a more idealized geometry of the North Atlantic. Winton et al. (1998) finally demonstrated that it is a resolution problem. When the resolution was high enough to resolve the bottom boundary layer and to resolve the slope, the flow is realistic enough. However, the required resolution is unrealistic even for modern z-models; therefore, they recommended the use of explicit bottom boundary layer models or the use of isopycnal models (although these also have their limitations, namely relating to disappearing layers and lack of vertical resolution in weakly stratified regions such as the deep mixed layer found in the winter season in the North Atlantic).

Shchepetkin and McWilliams (2003) developed a higher-order pressure gradient algorithm for σ-coordinate type models. When tested over an idealized seamount, they were able to diminish the errors. Similarly, a test application to the North Atlantic with a flat density field drastically reduced the spurious currents that arise from the non-alignment of the vertical pressure field with the horizontal. They also split the compressibility terms in a manner that allowed them to more accurately represent the physics without degrading the hydrostatic error.

From a different perspective, Hirst and McDougall (1996) noted that, in coarse resolution z-models, the Gent and McWilliams (1990) turbulence scheme remarkably enhances the conservation of water properties along topographic slopes. Another approach was proposed by Adcroft et al. (1997). They showed interesting use of "shaved" cells in z-models. The topography is then piecewise linear, instead of being piecewise constant at discrete levels as in typical z-models.

More recently, Chassignet et al. (2003) showed the viability of a hybrid vertical coordinate FD model based on ideas developed by Bleck and Boudra (1981) and Bleck and Benjamin (1993). The main goal of the hybrid vertical coordinate is to remedy the lack of vertical resolution of isopycnal models in critical locations such as deep mixed layers, i.e. the upper surface dynamics where the hybrid coordinate relaxes to a z-coordinate. Each hybrid level is essentially constrained to follow as much as possible an isopycnal surface unless it hits the mixed layer or the topography. This enables the use of more sophisticated parameterization of mixing in the mixed layer than the simple Kraus–Turner-type bulk formulae otherwise used in isopycnal-models (Treguier et al., 2005). Allowances were made as well to relax the hybrid coordinate to sigma coordinate on the shelves where resolving the bottom layer is crucial to the representation of vertical mixing. Whereas the isopycnal models tend to have too little diapycnal mixing, the hybrid coordinate would allow some in the boundary layers at the price that some spurious diapycnal mixing and pressure gradient errors may occur in steep topographic regions where the hybrid coordinate changes to another form.

High vertical resolution rarely leads to stability issues, as the vertical Courant number is usually small. Some exceptions may occur close to steep topography. For a hydrostatic model, this would correspond to a case where the hydrostatic approximation is probably no longer fully valid. Most models are hydrostatic, and generally speaking models treat the vertical diffusion implicitly due to the large value of the diffusion coefficients obtained from turbulence schemes. The vertical advection problem is usually treated explicitly in an Eulerian fashion. It is possible to treat the vertical advection problem implicitly which leads to the same tri-diagonal matrix problem as the one arising from the diffusion problem. However, this would give rise to an inconsistency in local conservation, with one advection problem being treated implicitly and one explicitly.

A possible stability limitation of z-levels models relates to the treatment of the free-surface. If the top layer is treated as having varying-depth, tides or atmospheric processes may create rapid variations in sea surface height (i.e. large vertical velocity) in the thin layers close to the surface. This problem is not present in sigma models for instance because the sigma velocity converges to zero as it gets close to the surface, whatever the variations in sea surface.

Ideally, a 3D circulation model should have enough vertical levels to represent the physics of the surface and bottom boundary layers where strong gradients are found with coarser resolution in between. The present state-of-the-art models with 40–50 levels are actually still behind these basic requirements.

10. Discussion

The resolution requirements described here can lead to multiple requirements in the different parts of a model. For example the consistent wavelength resolution (proportional to $\sqrt{gh}$) will give very different cell density over a shelf break from that needed to satisfy the resolution of steep slopes ($\Delta H/H$ small). Other differences with the criteria will of course be seen when there is high resolution in an area of particular interest. We expect the LTEA approach will see continued development and application with the ability to specify different error criteria for different regions depending on the focus of study.

Numerical models of coastal and shelf regions may be capable of capturing details of the flow in domains of interest, but they cannot afford to explicitly include the solution of the larger neighboring basin-scale domain. As such, regional models face a complication not found in global models namely the complexities of open boundaries. The transfer of energy into and out of the model domain via these boundaries can involve assumptions on the interaction of the modelled area with the adjacent unmodelled ocean. Frequently, the assumption is made that these boundaries are "small enough" and "far enough away" that the interactions do not impact the solution in the area of interest. However, establishing that this is the case remains a challenge. Variable resolution and nested grids or mapped coordinates are frequently used to help distance open boundaries from the principal area of interest.

The baroclinic Rossby radius of deformation is fundamentally related to the dynamics of global ocean circulation. It clearly needs to be resolved, but to what precision remains unclear. Improved model efficiencies and greater computer capacity have permitted models to move from resolutions of $>1^\circ \times 1^\circ$ (no eddies—Roberts et al., 2004) and $\frac{1}{3}^\circ \times \frac{1}{3}^\circ$ (eddy permitting—Gordon et al., 2000) to $0.1^\circ \times 0.1^\circ$ (approaching eddy resolving—Smith et al., 2000; Bryan et al., 2007; Maltrud and McClean, 2005). These latter simulations at $0.1^\circ$are beginning to reasonably reproduce fundamental eddy characteristics of the circulation. In part, this is attributed to better resolution of λ_1, even though this radius is at best minimally resolved in important parts of the model domains.

The occurrence of step-like features along the coastline of finite difference (FD) models is inevitable when modelling the real ocean. Curvilinear grids allow some flexibility in following the large scale features of the coastlines but do not prevent steps from occurring at small scales. A known effect of steps at coarse resolution in inviscid flows is to retard the propagation of waves along the model boundary. However, at higher resolution the problem disappears. In a circular domain, we found that FD models of different convergence order tend to be first-order only, which explains the retardation effect.

In presence of winds and viscous stresses, the free-slip boundary condition is problematic and yields solutions converging to too viscous circulations. A remedy found by Adcroft and Marshall (1998) was to replace the conventional viscous stress formulation based on the five-point Laplacian operator by a divergence–vorticity stress formulation. Note, however, that this solution is only applicable in situations where the steps are known to be artificial. Dupont (2001), in his thesis, reports problems when using this approach to the more general case of an undulating but otherwise circular basin. Therefore, the no-slip boundary condition seems to be more adequate in FD models even though the assumption that no-slip applies to large scale flows is not well justified.

The issues of vertical resolution have only briefly been touched upon here. The problems are complex, but different solutions are showing some promise. Hybrid vertical coordinates have the ability to avoid the larger diapycnal diffusion seen in z-level models and to increase the resolution in weakly stratified regions, which have been the main drawbacks of isopycnal models, while the interior of much of the ocean remains isopycnal (Chassignet et al., 2003). Similarly, using higher order equations to compute horizontal gradients in terrain following coordinate models may alleviate problems seen in this type of computation (Shchepetkin and McWilliams, 2003).

In the context of tidal data assimilation, it was found that in coarse models the absence of important dissipative and/or resonant estuaries was detrimental to the accuracy of the assimilated solution away from the location of the observations. Modellers interested in using data assimilation techniques in models with omitted/underesolved, but nonetheless potentially significant, portions of the focussed region need to be aware of this.

There have been recent investigations where mesh generation is part of the model, with resolution being increased or decreased on the basis of some aspect of the dynamics included (Blayo and Debreu, 1998; Pain et al., 2005; Gorman et al., 2006). So far these adaptive mesh models have been tested in idealized cases and for particular processes. This flexibility comes at the expense of very large computer demands.

10.1. Resolution issues—a list

Our review has covered several resolution issues that can affect the adequacy of model solutions. Briefly, these are:

(1) *Small scale processes* that interact with the large scale circulation need to be resolved if they cannot be parameterized.
(2) *Model coastlines* need to accurately represent the variations that can reflect and modify the coastal trapped motions.
(3) *Channels and sills* [*barotropic*] need cross sectional area and depth resolved to get the current phase speed and transport correct.
(4) *Channels and sills* [*baroclinic*] need the sill height accurately represented to get the right volume and density of overflow waters.
(5) *Topography* needs to be resolved. Convergence is enhanced with grid resolution matching wave speed. Steep bottom slopes need special attention to ensure that the change in depth over a grid cell ($\Delta H/H$) is small.
(6) *The baroclinic Rossby radius* needs to be resolved at some level to properly reproduce large scale ocean dynamics. As one approaches the poles, this could be a challenge.
(7) *Open boundary specification* of regional models will always require proper justification. Variable resolution and nested grid models can be used to move boundaries further from the domain of interest.
(8) *Assimilation* requires an understanding of the physics being modified to avoid using data to attempt to correct an improperly resolved solution.
(9) *Mesh generation* techniques are still developing and can now be used to meet specific model requirements.

11. Concluding remarks

The above discussion would appear to imply that the ocean modelling community is facing an impossible task in trying to meet all the requirements as outlined here. It seems clear that the use of unstructured grids may provide a better opportunity to resolve channels, sills, coastlines, critical slopes and localized areas of interest. However, even with this flexibility, these requirements are often not met, requiring additional advances in approaches such as adaptive mesh refinement (e.g. Blayo and Debreu, 1998, among others). However, all classes of circulation models have continued to provide robust solutions even with less than perfect numerics. As an example, Arakawa and Lamb (1981) have described techniques for properly accounting for the energy in non-linear models. The techniques are complicated and expensive to implement. Many models do not follow such a methodology yet still produce reliable answers to the questions posed.

Resolution is but one of the factors that comes into play when one chooses a model to apply to a particular application. Other dominant factors include stability, convergence and efficiency. A model's deficiency in any of these could quickly eliminate it from application to different problems. When the above are satisfactory, other factors such as available expertise and model support infrastructure can be considered. This paper predominantly addresses just one of these critical factors—resolution. We hope that this review will help the modeller identify weaknesses in solutions and enable more robust model design and discretization. Similarly, it is hoped that non-modellers, who use "off the shelf" modelling packages as basic tools, will do so aware of some the many issues that remain to be resolved.

Acknowledgments

We would like to thank Brian Blanton and Rick Luettich (University of North Carolina) for providing Figs. 9 and 10 and Scott Hagen (University of Central Florida) and coauthors for permission to use their work in Fig. 17. We also benefited from input from Joannes Westerink (Notre Dame), Keston Smith (Dartmouth College) and Jason Chaffey (Bedford Institute of Oceanography). F.E. Werner acknowledges support from the SEACOOS project.

References

Adcroft, A., Marshall, D., 1998. How slippery are piecewise-constant coastlines in numerical ocean models? Tellus 50A, 95–108.

Adcroft, A., Hill, C., Marshall, D., 1997. Representation of topography by shaved cells in a height coordinate ocean model. Monthly Weather Review 125, 2293–2315.

Alford, M.H., 2003. Redistribution of energy available for ocean mixing by long-range propagation of internal waves. Nature 423 (6936), 159–162.

Arakawa, A., Lamb, V.R., 1981. A potential enstrophy conserving scheme for shallow water equations. Monthly Weather Review 109 (1), 18–36.

Beletsky, D., O'Connor, W.P., Schwab, D.J., Dietrich, D.E., 1997. Numerical simulation of internal Kelvin waves and coastal upwelling fronts. Journal of Physical Oceanography 27, 1197–1215.

Bilgili, A., Smith, K., Lynch, D., 2005. Battri: a two-dimensional bathymetry-based unstructured triangular grid generator for finite element circulation modeling. Computers and Geosciences 32 (5), 632–642.

Blain, C., Westerink, J., Luettich, R., 1998. Grid convergence studies for the prediction of hurricane storm surge. International Journal for Numerical methods in Fluids 26, 369–401.

Blanton, B., Werner, F., Seim, H., Luettich Jr., R., Lynch, D., Smith, K., Voulgaris, G., Bingham, F., Way, F., 2004. Barotropic tides in the South Atlantic Bight. Journal of Geophysical Research 109 (C12), C12024.

Blayo, E., Debreu, L., 1998. Adaptive mesh refinement for finite difference ocean models: first experiments. Journal of Physical Oceanography 29, 1239–1250.

Blayo, E., Debreu, L., 2005. Revisiting open boundary conditions from the point of view of characteristic variables. Ocean Modelling 9, 231–252.

Bleck, R., 1978. Simulation of coastal upwelling frontogenesis with an isopycnic coordinate model. Journal of Geophysical Research 83, 6163–6172.

Bleck, R., Benjamin, S., 1993. Regional weather prediction with a model combining terrain-following and isentropic coordinates. Part I: model description. Monthly Weather Review 121, 1770–1785.

Bleck, R., Boudra, D.B., 1981. Initial testing of a numerical ocean circulation model using a hybrid quasi-isopycnal vertical coordinate. Journal of Physical Oceanography 11, 755–770.

Blumberg, A., Herring, H., 1987. Circulation modelling using orthogonal curvilinear coordinates. In: Nihoul, J., Jamart, B. (Eds.), Three-Dimensional Models of Marine and Estuarine Dynamics, Elsevier Oceanography, vol. 45. Elsevier, Amsterdam, pp. 55–88.

Blumberg, A., Kantha, L., 1985. Open boundary condition for circulation models. Journal of Hydraulic Engineering 111, 237–255.

Blumberg, A., Mellor, G., 1983. Diagnostic and prognostic numerical circulation studies of the South Atlantic Bight. Journal of Geophysical Research 88, 4579–4592.

Blumberg, A., Herring, H., Kantha, L., Mellor, G., 1985. 3-D orthogonal curvilinear circulation modelling. In: Hydraulics and Hydrology in the Small Computer Age. Hydraulics Division, ASCE, Lake Buena Vista, FL, August 12–17, pp. 1088–1094.

Blumberg, A., Signell, R., Jenter, H., 1993. Modelling transport processes in the coastal ocean. Journal of Marine Environmental Engineering 1, 31–52.

Bryan, F.O., Hecht, M.W., Smith, R.D., 2007. Resolution convergence and sensitivity studies with North Atlantic circulation models. Part I: the western boundary current system. Ocean Modelling 16, 141–159.

Bryan, K., 1969. A numerical method for the study of the circulation of the world ocean. Journal of Computational Physics 4, 347–376.

Camerlengo, A.L., O'Brien, J.J., 1980. Open boundary conditions in rotating fluids. Journal of Computational Physics 35 (1), 12–35.

Carey, G., 1995. Mesh generation, a posteriori error estimation, and mesh refinement. In: Lynch, D.R., Davies, A.M. (Eds.), Quantitative Skill Assessment for Coastal Ocean Models. Coastal and Estuarine Series, vol. 47. American Geophysical Union, Washington, DC, pp. 15–29.

Chapman, D., 1985. Numerical treatment of cross-shelf open boundaries in a barotropic coastal ocean model. Journal of Physical Oceanography 15 (8), 1060–1075.

Chassignet, E.P., Smith, L.T., Halliwell, G.R., 2003. North Atlantic simulations with the hybrid coordinate ocean model (HYCOM): impact of the vertical coordinate choice, reference pressure and thermobaricity. Journal of Physical Oceanography 33, 2504–2526.

Chelton, D.B., deSzoeke, R.A., Schlax, M.G., Naggar, K.E., Siwertz, N., 1998. Geographical variability of the first-baroclinic Rossby radius of deformation. Journal of Physical Oceanography 28, 433–460.

Cornillon, P., 1986. The effect of the New England Seamounts on Gulf Stream meandering as observed from satellite IR imagery. Journal of Physical Oceanography 16, 386–389.

Cox, M.D., 1979. A numerical study of Somali Currents eddies. Journal of Physical Oceanography 29, 311–326.

Cushman-Roisin, B., 1994. Introduction to Geophysical Fluid Dynamics. Prentice-Hall, New Jersey.

Davies, A.M., Hall, P., 2002. Numerical problems associated with coupling hydrodynamic models in shelf edge regions: the surge event of February 1994. Applied Mathematical Modelling 26, 807–831.

Davies, A.M., Xing, J., Gjevik, B., 2003. Barotropic eddy generation by flow instability at the shelf edge: sensitivity to open boundary conditions, inflow and diffusion. Journal of Geophysical Research 108 (C2), 17-1–17-15.

Dietrich, D.E., 1998. Application of a modified A-grid ocean model having reduced numerical dispersion to the Gulf of Mexico fronts circulation. Dynamics of Atmospheres and Oceans 27, 201–217.

Dupont, F., 2001. Comparison of numerical methods for modelling ocean circulation in basins with irregular coasts. Ph.D. Thesis, McGill University, Montreal, Canada.

Dupont, F., Petrie, B., Chaffey, J., 2003a. Modelling the tides of the Bras d'Or Lakes. Canadian Technical Report of the Hydrogen Ocean Science 230 Fisheries and Oceans Canada, Bedford Institute of Oceanography, Dartmouth, Nova Scotia.

Dupont, F., Straub, D.N., Lin, C.A., 2003b. Influence of a step-like coastline on the basin scale vorticity budget of mid-latitude gyre models. Tellus 55A (3), 255–272.

Dupont, F., Hannah, C.G., Wright, D.G., 2006. Model investigation of the slope water, north of the Gulf Stream. Geophysical Research Letters 33 (L05604).

Ezer, T., 1994. On the interaction between the Gulf Stream and the New England Seamount Chain. Journal of Physical Oceanography 24, 191–204.

Flather, R., 1981. Results from a model of the northeast Atlantic relating to the Norwegian Coastal Current. In: Saetre, R., Mork, M. (Eds.), The Norwegian Coastal Current, vol. 2. Bergen, Norway, pp. 427–458.

Foreman, M.G.G., 1984. A two-dimensional dispersion analysis of selected methods for solving the linearized shallow water equations. Journal of Computational Physics 56 (2), 287–323.

Foreman, M.G.G., Thomson, R.E., Smith, C.L., 2000. Seasonal current simulations for the western continental margin of Vancouver Island. Journal of Geophysical Research 105 (C8), 19665–19698.

Garrett, C., Greenberg, D., 1977. Predicting changes in tidal regime: the open boundary problem. Journal of Physical Oceanography 7 (2), 171–181.

Garrett, C., Toulaney, B., 1979. A variable-depth Green's function for shelf edge tides. Journal of Physical Oceanography 9, 1258.

Gent, P.R., McWilliams, J.C., 1990. Isopycnal mixing in ocean circulation models. Journal of Physical Oceanography 20, 150–155.

Gerdes, R., 1993. A primitive equation ocean general circulation model using a general vertical coordinate transformation. Journal of Geophysical Research 98, 14683–14701.

Gille, S.T., Metzger, E.J., Tokmakian, R., 2004. Seafloor topography and ocean circulation. Oceanography 17 (1), 47–54.

Gordon, C., Cooper, C., Senior, C.A., Banks, H., Gregory, J.M., Johns, T.C., Mitchell, J.F.B., Wood, R.A., 2000. The simulation of SST, sea ice extents and ocean heat transports in a version of the Hadley Centre coupled model without flux adjustments. Climate Dynamics 16 (2–3), 147–168.

Gorman, G., Piggott, M., Pain, C., de Oliveira, C., Umpleby, A., Goddard, A., 2006. Optimisation based bathymetry approximation through constrained unstructured mesh adaptivity. Ocean Modelling 12, 436–452.

Greenberg, D.A., 1979. A numerical model investigation of tidal phenomena in the Bay of Fundy and Gulf of Maine. Marine Geodesy 2 (2), 161–187.

Greenberg, D.A., Shore, J.A., Page, F.H., Dowd, M., 2005. A finite element circulation model for embayments with drying intertidal areas and its application to the Quoddy region of the Bay of Fundy. Ocean Modelling 10, 211–231.

Hagen, S., 2001. Estimation of the truncation error for the linearized shallow water momentum equations. Engineering with Computers 17, 354–362.

Hagen, S., Parrish, D., 2003. Meshing requirements for tidal modeling in the western North Atlantic. International Journal of Computational Fluid Dynamics 18 (7), 585–595.

Hagen, S., Westerink, J., Kolar, R., 2000. One-dimensional finite element grids based on localized truncation error analysis. International Journal for Numerical Methods in Fluids 32, 241–261.

Hagen, S., Westerink, J., Kolar, R., Horstmann, O., 2001. Two dimensional unstructured mesh generation for tidal models. International Journal for Numerical Methods in Fluids 35, 669–686.

Hagen, S.C., Horstmann, O., Bennett, R.J., 2002. An unstructured mesh generation algorithm for shallow water modeling. International Journal of Computational Fluid Dynamics 16 (2), 83–91.

Haidvogel, D., Wilkin, J., Young, R., 1991. A semi-spectral primitive equation ocean circulation model using vertical sigma and orthogonal curvilinear horizontal coordinates. Journal of Computational Physics 94, 151–185.

Haidvogel, D.B., Beckmann, A., 1999. Numerical Ocean Circulation Modeling. Imperial College Press, London.

Hall, P., Davies, A.M., 2005a. Comparison of finite difference and element models of internal tides on the Malin-Hebrides shelf. Ocean Dynamics 55, 272–293.

Hall, P., Davies, A.M., 2005b. Effect of coastal boundary resolution and mixing upon internal wave generation and propagation in coastal regions. Ocean Dynamics 55, 248–271.

Haney, R.L., 1991. On the pressure gradient force over steep topography in sigma coordinate ocean models. Journal of Physical Oceanography 21, 610–619.

Hannah, C.G., Wright, D.G., 1995. Depth dependent analytical and numerical solutions for wind-driven flow in the coastal ocean. In: Lynch, D.R., Davies, A.M. (Eds.), Quantitative Skill Assessment for Coastal Ocean Models. Coastal and Estuarine Studies, vol. 47. AGU, Washington, DC, pp. 125–152.

Hayashi, T., Greenberg, D., Garrett, C., 1986. A note on open boundary conditions for numerical models of shelf circulation. Continental Shelf Research 5 (4), 487–497.

Haza, A.C., 2004. Study of the gulf stream-slopewater system. Ph.D. Thesis, University of Miami, Miami, Florida.

Henry, R., Walters, R., 1993. Geometrically based, automatic generator for irregular triangular networks. Numerical Methods in Engineering 9, 555–566.

Hermann, A., Haidvogel, D.B., Dobbins, E.L., Stabeno, P.J., 2002. Coupling global and regional circulation models in the coastal gulf of alaska. Progress in Oceanography 53, 335–367.

Hirst, A., McDougall, T.J., 1996. Deep-water properties and surface buoyancy flux as simulated by a z-coordinate model including eddy-induced advection. Journal of Physical Oceanography 26, 1320–1343.

Hua, B., Thomasset, F., 1984. A noise free finite element scheme for the two layer shallow equations. Tellus, 157–165.

Johnsen, M., Lynch, D., 1995. Assessment of a second-order radiation boundary condition for tidal and wind-driven flows. In: Lynch, D., Davies, A. (Eds.), Quantitative Skill Assessment for Coastal Ocean Models. Coastal and Estuarine Studies, vol. 47. American Geophysical Union, Washington, DC.

Jones, J.E., Davies, A.M., 2005. An intercomparison between finite difference and finite element (telemac) approaches to modeling west coast of Britain tides. Ocean Dynamics 55, 178–198.

Kantha, L., Clayson, C., 2000. Numerical models of Oceans and Oceanic Processes. International Geophysics, vol. 66. Academic Press, New York.

Kliem, N., Greenberg, D.A., 2003. Diagnostic simulations of the summer circulation in the Canadian Arctic Archipelago. Atmosphere-Ocean 41 (4), 273–289.

Laval, B., Imberger, J., Findikakis, A.N., 2003. Mass transport between a semi-enclosed basin and the ocean: Lake Maracaibo. Journal of Geophysical Research 108 (C7), 3234.

Le Provost, C., Genco, M.-L., Lyard, F., 1995. Modeling and predicting tides over the world ocean. In: Lynch, D.R., Davies, A.M. (Eds.), Quantitative Skill Assessment for Coastal Ocean Models. Coastal and Estuarine Series, vol. 47. American Geophysical Union, Washington, DC, pp. 175–201.

Loder, J.W., 1980. Topographic rectification of tidal currents on the sides of Georges Bank. Journal of Physical Oceanography 10, 1399–1416.

Luettich, R., Westerink, J., 1995. Continental shelf scale convergence studies with a barotropic tidal model. In: Lynch, D.R., Davies, A.M. (Eds.), Quantitative Skill Assessment for Coastal Ocean Models. Coastal and Estuarine Series, vol. 47. American Geophysical Union, Washington, DC, pp. 349–371.

Lyard, F., Lefevre, F., Letellier, T., Francis, O., 2006. Modelling the global ocean tides: a modern insight from FES2004. Ocean Dynamics 56, 394–415.

Lynch, D., 2005. Numerical Partial Differential Equations for Environmental Scientists and Engineers. Springer, New York.

Lynch, D., Hannah, C., 2001. Inverse model for limited-area hindcasts on the continental shelf. Journal of Atmospheric and Oceanic Technology 18, 962–981.

Lynch, D., Naimie, C., 2002. Hindcasting the Georges Bank circulation, part II: wind-band inversion. Continental Shelf Research 22, 2191–2224.

Lynch, D., Werner, F., Molines, J., Fornerino, M., 1990. Tidal dynamics in a coupled ocean–lake system. Estuarine, Coastal and Shelf Science 31, 319–343.

Lynch, D., Ip, J., Naimie, C., Werner, F., 1995. Convergence studies of tidally-rectified circulation on Georges Bank. In: Lynch, D., Davies, A. (Eds.), Quantitative Skill Assessment for Coastal Ocean Models, vol. 47. American Geophysical Union, pp. 153–174.

Lynch, D., Naimie, C., Hannah, C., 1998. Hindcasting the Georges Bank circulation, part: I detiding. Continental Shelf Research 18, 607–639.

Lynch, D., Naimie, C., Ip, J., Lewis, C., Werner, F., Luettich Jr., R.A., Blanton, B., Quinlan, J., McGillicuddy, D., Ledwell, J., Churchill, J., Kosnyrev, V., Davis, C., Gallager, S., Ashjian, C., Lough, R., Manning, J., Flagg, C., Hannah, C., Groman, R., 2001. Real-time data assimilative modeling on Georges Bank. Oceanography 14, 65–77.

Lynch, D.R., Holboke, M.J., 1997. Normal flow boundary conditions in 3d circulation models. International Journal for Numerical Methods in Fluids 25, 1185–1205.

Lynch, D.R., Werner, F.E., 1987. Three-dimensional hydrodynamics on finite elements. Part I: linearized harmonic model. International Journal for Numerical Methods in Fluids 7, 871–909.

Lynch, D.R., Werner, F.E., 1991. Three-dimensional hydrodynamics on finite elements. Part II: nonlinear time-stepping model. International Journal for Numerical Methods in Fluids 12, 507–533.

Lynch, D.R., Werner, F.E., Greenberg, D.A., Loder, J.W., 1992. Diagnostic model for baroclinic, wind-driven and tidal circulation in shallow seas. Continental Shelf Research 12, 37–64.

Lynch, D.R., Smith, K.W., Blanton, B.O., Luettich, R.A., Werner, F.E., 2004. Forecasting the coastal ocean: resolution, tide and operational data in the South Atlantic Bight. Journal of Oceanic and Atmospheric Technology 21 (7), 1074–1085.

Madec, G., Chartier, M., Delecluse, P., Crepon, M., 1991. A three-dimensional numerical study of deep-water formation in the northwestern Mediterranean Sea. Journal of Physical Oceanography 21, 1349–1371.

Maltrud, M.E., McClean, J.L., 2005. An eddy resolving global $1/10^{\circ}$ ocean simulation. Ocean Modelling 8, 31–54.

Mellor, G., Hakkinen, S., Ezer, T., Patchen, R., 2002. A generalization of a sigma coordinate ocean model and an intercomparison of model vertical grids. In: Pinardi, N., Woods, J. (Eds.), Ocean Forecasting: Conceptual Basis and Applications. Springer, Berlin, pp. 55–72.

Mellor, G.L., Ezer, T., Oey, L.Y., 1994. The pressure gradient conundrum of sigma coordinate ocean models. Journal of Atmospheric and Oceanic Technology 11, 1126–1134.

Metzger, E.J., Hurlburt, H.E., 2001. The importance of high horizontal resolution and accurate coastline geometry in modeling South China Sea inflow. Geophysical Research Letters 28 (6), 1059–1062.

Molines, J., Fornerino, M., le Provost, C., 1989. Tidal spectroscopy of a coastal area: observed and simulated tides of the Lake Maracaibo system. Continental Shelf Research 9 (4), 301–323.

Mysak, L.A., Tang, C.L., 1974. Kelvin wave propagation along an irregular coastline. Journal of Fluid Mechanics 64, 241–261.

Oey, L.-Y., Chen, P., 1992. A nested-grid ocean model: with application to the simulation of meanders and eddies in the Norwegian Coastal Current. Journal of Geophysical Research 97 (C12), 20,087–20,115.

Orlanski, I., 1976. A simple boundary condition for unbounded hyperbolic flows. Journal of Computational Physics 21, 251–269.

Pain, C., Piggott, M., Goddard, A., Fang, F., Gorman, G., Marshall, D., Eaton, M., Power, P., de Oliveira, C.R.E., 2005. Three-dimensional unstructured mesh ocean modelling. Ocean Modelling 10, 5–33.

Palma, E.D., Matano, R.P., 1998. On the implementation of passive open boundary conditions for a general circulation model: the barotropic mode. Journal of Geophysical Research 103 (C1), 1319–1341.

Pedersen, G., 1996. On the effect of irregular boundaries in finite difference models. International Journal for Numerical Methods in Fluids 6, 497–505.

Penduff, T., Barnier, B., de Verdière, A.C., 2000. Self-adapting open boundaries for regional models: application to the eastern North Atlantic. Journal of Geophysical Research 105, 11279–11297.

Peraire, J., Zienkiewicz, O.C., Morgan, K., 1986. Shallow water problems: a general explicit formulation. International Journal for Numerical Methods in Engineering 22, 547–574.

Petrie, B., 1999. Sea level variability in the Bras d'Or Lakes. Atmosphere-Ocean 37 (2), 221–239.

Petrie, B., Bugden, G., 2002. The physical oceanography of the Bras d'Or Lakes. Proceedings of the Nova Scotia Institute of Science 42 (1), 9–36.

Phillips, N.A., 1957. A coordinate system having some special advantages for numerical forecasting. Journal of Meteorology 14, 184–185.

Pickart, R.S., McKee, T.K., Torres, D.J., Harrington, S.A., 1999. Mean structure and interannual variability of the slopewater system south of Newfoundland. Journal of Physical Oceanography 29 (10), 2541–2558.

Platzman, G.W., 1975. Normal modes of the Atlantic and Indian Oceans. Journal of Physical Oceanography 5 (2), 201–221.

Richtmeyer, R., Morton, K., 1967. Difference Methods for Initial Value Problems. Interscience Publishers, New York.

Roache, P., 1976. Computational Fluid Dynamics. Hermosa Publishing, Albuquerque, NM.

Roberts, M.J., Wood, R.A., 1997. Topographic sensitivity studies with a Bryan–Cox type ocean model. Journal of Physical Oceanography 27, 823–836.

Roberts, M.J., Marsh, R., New, A.L., Wood, R.A., 1996. An intercomparison of a Bryan–Cox-type ocean model and an isopycnic ocean model. Part I: the subpolar gyre and high latitude processes. Journal of Physical Oceanography 26, 1495–1527.

Roberts, M.J., Banks, H.N.G., Gregory, J., Hill, R., Mullerworth, S., Pardaens, A., Rickard, G., Thorpe, R., Wood, R., 2004. Impact of an eddy-permitting ocean resolution on control and climate change simulations with a global coupled GCM. Journal of Climate 17 (1), 3–20.

Roed, L.P., Smedstad, O.M., 1984. Open boundary conditions for forced waves in a rotating fluid. SIAM Journal on Scientific and Statistical Computing 5 (2), 414–426.

Sadourny, R., 1975. The dynamics of finite difference models of the shallow water equations. Journal of Atmospheric Sciences 32, 680–689.

Schopf, P.S., Suarez, M.J., 1988. Vacillations in a coupled ocean–atmosphere model. Journal of Atmospheric Science 45, 549–566.

Schwab, D.J., Beletsky, D., 1998. Propagation of Kelvin waves along irregular coastlines in finite-difference models. Advances in Water Resources 22 (3), 239–245.

Shchepetkin, A.F., McWilliams, J.C., 2003. A method for computing horizontal pressure-gradient force in an oceanic model with a nonaligned vertical coordinate. Journal of Geophysical Research 108 (C3), 3090.

Smith, K., 2005. M2 tides and power generation in Vineyard Sound, Nantucket Sound, and Nantucket Shoals. Internal Report NML-05-10, Dartmouth College, Hanover, NH, USA.

Smith, R., Maltrud, M., Bryan, F., Hecht, M., 2000. Numerical simulation of the North Atlantic Ocean at $1/10^{\circ}$. Journal of Physical Oceanography 30, 1532–1561.

Soares, J., Wainer, I., Wells, N., 1999. Reflection of equatorial Kelvin waves at eastern ocean boundaries, part I: hypothetical boundaries. Annales Geophysicae 17, 812–826.

Song, Y., Haidvogel, D.B., 1994. A semi-implicit ocean circulation model using a generalized topography-following coordinate system. Journal of Computational Physics 115, 228–244.

Stammer, D., 1997. Global characteristics of ocean variability from regional TOPEX/POSEIDON altimeter measurements. Journal of Physical Oceanography 27, 1743–1769.

Treguier, A.M., Theetten, S., Chassignet, E.P., Penduff, T., Smith, R., Talley, L., Beismann, J.O., Böning, C., 2005. The North Atlantic subpolar gyre in four high-resolution models. Journal of Physical Oceanography 35, 757–774.

Werner, F.E., Blanton, J.O., Lynch, D.R., Savidge, D.K., 1993a. A numerical study of the continental shelf circulation of the U.S. South Atlantic Bight during autumn of 1987. Continental Shelf Research 13, 971–997.

Werner, F.E., Page, F.H., Lynch, D.R., Loder, J.W., Lough, R.G., Perry, R.I., Greenberg, D.A., Sinclair, M.M., 1993b. Influences of mean advection and simple behavior on the distribution of cod and haddock early life stages on Georges Bank. Fisheries Oceanography 2, 43–64.

Westerink, J., Luettich, R., Blain, C., Hagen, S., 1995. Surface elevation and circulation in continental margin waters. In: Carey, G. (Ed.), Finite Element Modeling of Environmental Problems. Wiley, Chichester, pp. 39–60.

Whitehead, J.A., 1998. Topographic control of oceanic flows in deep passages and straits. Reviews of Geophysics 36, 423–440.

Winton, M., 1997. The damping effect of bottom topography on internal decadal-scale oscillations of the thermohaline circulation. Journal of Physical Oceanography 27, 203–208.

Winton, M., Hallberg, R., Gnanadesikan, A., 1998. Simulation of density-driven frictional downslope flow in z-coordinate ocean models. Journal of Physical Oceanography 27, 2163–2174.

Wright, D.G., Loder, J.W., 1985. A depth-dependent study of the topographic rectification of tidal currents. Geophysical and Astrophysical Fluid Dynamics 31, 169–220.

Xing, J., Davies, A., 1997. The influence of wind effects upon internal tides in shelf edge regions. Journal of Physical Oceanography 27, 2100–2125.

Xing, J., Davies, A., 1998. A three-dimensional model of internal tides on the Malin-Hebrides shelf and shelf edge. Journal of Geophysical Research 103, 27,821–27,847.

Xing, J., Davies, A., 2001. Non-linear effects of internal tides on the generation of the tidal mean flow at the Hebrides shelf edge. Geophysical Research Letters 28 (20), 3939–3942.